

AMERICAN UNIVERSITY OF BEIRUT

DRAINED CLAY-PIPE INTERFACE RESISTANCE AT LOW
NORMAL STRESSES AND ELEVATED TEMPERATURES

by
MIRNA HASSAN BASMA

A thesis
submitted in partial fulfillment of the requirements
for the degree of Master of Engineering
to the Department of Civil and Environmental Engineering
of Maroun Semaan Faculty of Engineering and Architecture
at the American University of Beirut


Beirut, Lebanon
February 2022

AMERICAN UNIVERSITY OF BEIRUT

DRAINED CLAY-PIPE INTERFACE RESISTANCE AT LOW
NORMAL STRESSES AND ELEVATED TEMPERATURES

by
MIRNA HASSAN BASMA

Approved by:



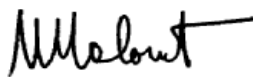
Dr. Shadi Najjar, Associate Professor
Department of Civil and Environmental Engineering

Advisor



Dr. Salah Sadek, Professor
Department of Civil and Environmental Engineering

Co-Advisor



Dr. Mounir Mabsout, Professor
Department of Civil and Environmental Engineering

Member of Committee

Date of thesis defense: February 2022

AMERICAN UNIVERSITY OF BEIRUT

THESIS RELEASE FORM

Student Name: Basma Mirna Hassan
Last First Middle

I authorize the American University of Beirut, to: (a) reproduce hard or electronic copies of my thesis; (b) include such copies in the archives and digital repositories of the University; and (c) make freely available such copies to third parties for research or educational purposes:

- As of the date of submission
- One year from the date of submission of my thesis.
- Two years from the date of submission of my thesis.
- Three years from the date of submission of my thesis.



May 12, 2022

Signature

Date

ACKNOWLEDGEMENTS

Throughout the writing of this thesis, I have received kind support and assistance by many.

First and foremost, praises and thanks to God, the Almighty, for granting me this opportunity and blessing to be able to finish my research successfully.

I would like to express my deepest appreciation to my advisors Dr. Shadi Najjar and Dr. Salah Sadek, whose expertise were invaluable in formulating the research. Their insightful feedbacks brought my work to a higher level. Thank you for your unwavering guidance over the past two years.

I would also like to thank Dr. Mounir Mabsout for being a member of my thesis committee along with my advisors and for reviewing my work.

The completion of my thesis would not have been possible without the support of Dr. Roba Houhou who is considered a big part of this research study.

I'm also deeply indebted to my colleagues for extending a great amount of assistance and for their help throughout my experimental campaign.

Special thanks to the geotechnical engineering laboratory managers Mr. Helmi Al-Khatib and Ms. Dima Al Hassanieh for their insightful and rational suggestions every time we encounter a technical problem.

Finally, I'm extremely grateful to my family and friends for always believing in my abilities and for providing me with encouragement throughout the duration of this research. This accomplishment would not have been possible without you.

ABSTRACT OF THE THESIS OF

Mirna Hassan Basma

for

Master of Engineering

Major: Civil and Environmental Engineering

Title: Drained Clay-Pipe Interface Resistance at Low Normal Stresses and Elevated Temperatures

Offshore pipelines transport hydrocarbons under high pressure and high temperature conditions in order to improve/control their flowability. These pipelines are usually thermally insulated to maintain an elevated temperature and prevent any heat loss to the surroundings. However, the temperatures at the outer-wall of the pipes may still be elevated and therefore potentially altering the interface resistance between the pipeline and the seabed. This study aims at experimentally investigating the drained shear resistance at the soil-pipe interface at elevated temperatures and low normal stress conditions typical of field conditions. A series of direct shear tests are performed using a modified-for purpose direct shear apparatus that allows for very low confinement stresses and the control of interface temperatures. Low and high plasticity clays are consolidated from a slurry and sheared against smooth and rough interfaces to characterize the peak and residual interface shear response under drained loading conditions. The modified shear test apparatus is equipped with a heating circulator that allowed for the sustained control of temperatures at the soil-pipe interface to the desired levels: 22°C and 60°C for the temperatures used in this study. Results indicated that the effect of elevated temperature on the interface resistance is highly complex and dependent on the roughness of the pipe coating, the plasticity of the clay, and the magnitude of the applied normal stress. For low plasticity clay, the smooth coating showed increases in peak and residual interface strength at elevated temperatures while the tests conducted with rough coatings indicated reductions in interface strength at elevated temperatures. For high plasticity clays, an opposite trend was observed with elevated temperatures causing a decrease in the peak strength for the smooth interface and a slight increase for the rough interface. The residual strength was however reduced in both types of interfaces at elevated temperature. These results are important and necessitate further interface testing at elevated temperatures in the low pressure range to cover the wide spectrum of combinations of clay plasticity and pipe roughness that may exist in practice.

TABLE OF CONTENTS

ACKNOWLEDGEMENTS	1
ABSTRACT	2
ILLUSTRATIONS	5
TABLES	7
ABBREVIATIONS	8
INTRODUCTION	10
A. Characteristic Parameters of the Axial Pipe-Soil Interaction	11
B. Temperature Effect	12
REVIEW OF LITERATURE.....	16
A. Lab Element Testing of Interface Resistance at Low Confinement Stresses	16
B. Thermal Effect on Interface Resistance.....	18
MATERIALS AND METHODS	32
A. Description of the Modified Direct Shear Apparatus	32
B. Materials	35
1. Soil.....	35
2. Interface Material.....	37
C. Test Procedure	39
D. Setup Calibration	40

EXPERIMENTAL RESULTS	43
A. Consolidation Phase.....	43
B. Heating Phase	44
C. Shearing Phase	46
1. Effect of Temperature on Interface Response	47
a. Low Plasticity Clay (LPC).....	47
b. High Plasticity Clay (HPC).....	54
2. Effect of Pipe Roughness on the Mode of Failure	56
3. Effect of Clay Plasticity and Temperature on the Residual Friction Angle ...	57
 CONCLUSIONS	 60
 REFERENCES	 62

ILLUSTRATIONS

Figure

1. GDS Direct Shear device (Di Donna et al., 2016) - 1, GDSLAB software control, 2, normal actuator, 3, horizontal actuator, 4, LVDTs, acquisition pad, 5, load cells, 6, LVDTs, 7, specimen placement, 8, top cap, and 9, axial piston ...	20
2. Effect of temperature on shear strength of (a) sand-concrete interface and (b) clay-concrete interface (Di Donna et al., 2016).....	21
3. Direct shear apparatus with temperature control system (Yavari et al., 2016)...	22
4. Effect of temperature on (a) friction angle and (b) cohesion.....	22
5. (a) Schematic diagram of new Direct Shear apparatus and (b) temperature monitoring sensors (Wang et al., 2018).....	23
6. Impacts of thermal loads in the (a) sand-concrete and (b) clay-concrete interface tests on the net normal stress in relation to shear strength.....	23
7. Schematic view of modified direct shear apparatus (b) Layout of the heating/cooling tubing in the concrete plate. (Yazdani et al., 2019)	24
8. Effect of (a) interface normal stress, and (b) stress history of clay (OCR) on the thermo-mechanical response of interface (Yazdani et al., 2019)	24
9. Modified Direct Shear test device (Xiao et al., 2017)	25
10. Shear stress-displacement curves of soil-concrete interface under different normal stresses (27.6, 41.4, and 100 kPa) (Xiao et al., 2017)	25
11. Direct shear apparatus in temperature-controlled chamber (C. Li et al., 2019) .	26
12. Failure envelopes of red clay–geostructure at different temperatures	27
13. Experimental setup of the direct shear temperature-controlled device (Maghsoodi et al., 2019).....	27
14. Shear stress vs. effective normal stress of CNL tests of clay-structure interface at different temperatures	28
15. Effect of normalized roughness on sand-steel interface response under CNL conditions (a) shear strength and (b) vertical deformation, as a function of relative tangential displacement (Hu & Pu, 2004).....	30
16. Shear stress vs. shear displacement of clay-concrete interface for different roughness (Shakir & Zhu, 2009).....	30
17. Mohr-Coulomb envelopes of clay-concrete interfaces (Chen et al., 2015).....	30
18. Classification of failure modes (Tsubakihara et al., 1993).....	31
19. Modified direct shear setup.....	33

20. (a) Schematic drawing and (b) real image of copper tubes configuration in lower box	34
21. Water supplier	34
22. (a) Natural Clay with low plasticity (LPC) and (b) High Plasticity Clay (HPC)	35
23. Grain-size distribution of (a) LPC and (b) HPC	36
24. 100x90mm Stainless steel sheets	37
25. 100x90mm Sandpaper sheets.....	37
26. Profilometer readings for Stainless steel	38
27. Profilometer readings for Sandpaper	38
28. SEM images of (a) LPC, (b) HPC, (c) KAO, (d) Plexiglass, (e) Stainless Steel, and (f) Sandpaper.....	39
29. Friction and Temperature Effects on Shear Stresses for (a) Stainless Steel and (b) Sandpaper	41
30. Vertical displacement due to elevated temperature	41
31. (a) Location of thermocouples (b) Temperature variation at different locations in shear box	42
32. Consolidation curves at normal stresses of 2.45, 4.26, and 6.1kPa	44
33. Vertical displacement vs. time from the start of heating	45
34. Interface response during direct shear testing at ambient temperature (22°C) and elevated temperature (60°C) for (a) LPC with Steel and (b) LPC with Sandpaper	50
35. Variation of peak shear stress, residual shear stress, peak friction angle, and residual friction angle with normal stress for (a) LPC with Steel and (b) LPC with Sandpaper	51
36. Interface response during direct shear testing at ambient temperature (22°C) and elevated temperature (60°C) (a) HPC with Steel and (b) HPC with Sandpaper.	52
37. Variation of peak shear stress, residual shear stress, peak friction angle, and residual friction angle with normal stress for (a) HPC vs Steel and (b) HPC vs Sandpaper.....	53
38. Failure mechanism of LPC on (a) Stainless steel and (b) Sandpaper	57
39. Failure mechanism of HPC on (a) Stainless steel and (b) Sandpaper	57
40. Residual Secant Friction Angle for (a) LPC and (b) HPC.....	58

TABLES

Table

1. Element testing devices for measuring interface shear resistance (Westgate et al., 2018a)	17
2. Summary of published experimental studies for interface testing in geothermal foundations.....	19
3. Effect of temperature on interface shear parameters for sandy silty clay (Xiao et al., 2017)	26
4. Minimum Standing Time for Samples prepared.....	36
5. Normal Stress Corrections due to Friction	42
6. Testing Program for Interface Direct Shear tests.....	47

ABBREVIATIONS

HPHT: High pressure high temperature

LPC: Low plasticity clay

HPC: High plasticity clay

SS: Stainless steel

LVDT: linear variable differential transformer

CNL: Constant normal load

The thesis plan is described in detail in the following.

Chapter I: A brief definition of offshore pipelines, the characteristic parameters of axial pipeline-soil interaction, and the evolution of engaging temperature effect in geotechnical engineering researches.

Chapter II: This chapter holds the literature review where the main titles discussed are, lab element testing of interface resistance at low confinement stresses as well as the thermal and structure roughness effect on interface resistance.

Chapter III: A detailed description of all the materials used in this study is presented. The modified direct shear device is showed in detail and all developments in the device are tackled. Sample preparation and experimental program are also discussed in this chapter. And finally, the setup calibration tests are presented.

Chapter IV: In this chapter, the effect of temperature on the mechanical behavior of the clay-pipeline interface is studied. A testing program is proposed to investigate the shear characteristics of soil-structure interface at 60°C and compared to reference tests at 22°C under constant normal stress levels (CNL). At the end, the effect of temperature on shear stress-displacement and volumetric behavior is discussed. The effect of structure roughness and the failure mechanisms are also reviewed.

Chapter V: Conclusions are drawn in this chapter.

CHAPTER I

INTRODUCTION

Offshore pipelines are critical elements of the subsea system for the transportation and delivery of hydrocarbon products from source to destination. Subsea pipelines are increasingly being required to operate at high temperature and pressure HTHP. Modern technology of pipeline construction and utilization under extreme operating conditions has achieved unquestionable success. Yet, the pipeline's integrity might be impaired during transporting hydrocarbons. HPHT pipelines experience expansion and contraction due to changes in internal temperature and pressure. These movements are opposed by the pipe-seabed axial resistance. The pipeline is then susceptible to buckling and walking under thermal gradients during startup and shutdown events. This could lead to failure of the pipeline itself or the end connections if buckling and walking are not properly controlled or mitigated. As such, an accurate estimation of the axial pipe-soil interaction resistance is inevitable to safely design offshore pipelines and prevent any risk associated with the buckling and walking phenomena.

According to (Boulon, 1989) and (Uesugi & Krshida, 1987), soil-structure interface is defined as a thin zone of soil which has quite different mechanical properties from the rest of the soil. Targeted research studies in the last two decades have attempted to characterize and model the response of the soil at the pipe interface. However, accurate measurements of the interface's thickness are still poorly described despite recent studies that aimed at identifying, measuring, and evaluating the soil-structure interface thickness. These limited studies are based on new visualization

techniques. For instance, Particle Image Velocimetry (PIV), Digital Image Correlation (DIC) technique, and high-resolution photography method can be used to visualize the interface zone deformation and to measure the interface thickness (Yin et al., 2021), which has been found to be a multiple of the average particles diameter depending on the properties of soil and structure.

A. Characteristic Parameters of the Axial Pipe-Soil Interaction

During the last two decades, significant research efforts have been dedicated to characterize the axial interface resistance between the pipelines and the seabed. Many parameters have been found to influence this resistance as listed in the following points (Westgate et al., 2018b):

- 1. Soil properties:** strength parameters (cohesion and friction angles), permeability, consolidation coefficient
- 2. Normal stress level:** relating to the bearing pressure imposed by the pipeline onto the seabed
- 3. Overloading history:** or changes in the bearing pressure due to pipeline contents changes through commissioning and operation (which can create an overconsolidation of the soil at the pipeline-seabed interface)
- 4. Pipeline coating roughness:** depending on the coating type used for offshore pipelines and can range from smooth to rough
- 5. Drainage conditions:** related to the duration of axial pipeline movement during startup or shutdown events (which affects the level of drainage during the movement)

6. **Pause periods between operations:** Duration of pipeline rest between startup and shutdown events (which affects the level of drainage between movements)
7. **Pipeline embedment:** via the ‘wedging’ factor that enhances the normal contact force to exceed the pipe weight.

Recent studies and models focused on showing the effect of each of these parameters on the interface resistance throughout its operational life using different testing techniques, which include laboratory element tests (Boukpeti & White, 2016; Brier et al., 2016; Eid et al., 2015; S. S. Najjar et al., 2007; Shadi S Najjar et al., 2003; Pedersen et al., 2019; Randolph et al., 2012; Westgate et al., 2018b) , model tests (Boylan & White, 2014; Shi et al., 2019) and in-situ tests (Ballard & Jewell, 2013; Hill & Jacob, 2008; Stanier et al., 2015).

A main parameter that was not accounted for in all the aforementioned studies is the temperature at the interface. In fact, offshore pipelines operate at high temperature which may affect the resistance between these pipelines and the seabed. Recently, the effect of temperature on the soil and the interface behavior have been widely studied especially in the field of geothermal structures. This topic is covered in the next chapter.

B. Temperature Effect

The possible effect of temperature change on the geotechnical properties of soil has become a key factor in several engineering designs and applications. Engaging temperature in researches started in the 20th century when researchers were interested in finding a relationship between laboratory temperature and actual field temperature and its effect on soil properties. The first international conference presenting the

influence of temperature and heat on the engineering behavior of soils was held at Washington D.C, January 1969.

Gray (1936) was the first to conduct an oedometer test at different temperatures. The result of altering the temperature indicated that an increase in temperature resulted in a higher rate of secondary consolidation (Gray, 1936; Lo, 1961; Schiffman, et al., 1966). Richard Kai-Ming (Richard Kai-Ming, 1971) also concluded that an increase of temperature during secondary consolidation may cause weakened bonds and a rearrangement of particles. Paaswell (Paaswell, 1967) adapted a consolidometer to provide temperature changes through a heating element and measured the quantity of deformation induced by increasing boundary temperatures at a given stress level and noticed that the magnitude of the resulting deformation depended directly on the magnitude of the temperature increase.

More complicated engineering applications started to arise with advancing technology. This vitalized researchers to show extensive understanding of the behavior of soil at elevated temperatures. Several applications today involve temperature that can alter the soil strength, such as geothermal foundation engineering (Houhou et al., 2018), radioactive waste disposal (Delage et al., 2010), deep geothermal reservoirs (Ozgener et al., 2013), and offshore pipeline construction (H. Li et al., 2020).

In the context of geothermal foundation engineering, many studies have been conducted to assess the influence of temperature change on soil-structure interface behavior for energy piles. Different structural materials were tested under relatively high normal stresses ranging between 50 and 400 kPa and different temperatures (2-60°C). The studies were conducted using the modified temperature-controlled direct shear apparatus, where sand and clay were tested against different structural materials.

Other studies focused on the effect of temperature on the soil itself. It is well known now that the volume change due to temperature tends to be contractive for normally consolidated (NC) clays, whereas it becomes expansive for highly overconsolidated (OC) clays (Cekerevac & Laloui, 2004). A slightly overconsolidated clay, though, is expected to first dilate, then with further heating contract.

Offshore pipelines likewise are subjected to thermal loadings as they operate at high temperatures and high pressures. So far, researchers have focused on understanding the interface behaviour at low normal stresses without considering the temperature variations. However, it has been demonstrated that the outer surface temperature of HPHT pipelines can reach 55°C (Bai et al., 2014) which may eventually alter the interface resistance as proven earlier. Accordingly, the effect of temperature on the mechanical parameters of the pipe-soil interface should be considered.

During the last few decades, the understanding of offshore pipeline behaviour has improved significantly. Important efforts have been made to reliably estimate the pipeline axial resistance throughout the pipeline's operational life using different testing techniques, which include laboratory element tests, model tests, and in-situ tests. Among the published work on measuring the axial resistance, there has been very few attempts to include temperature effect in the study.

The proposed work aims at determining the drained clay-pipe interface resistance at low normal stresses and elevated temperatures simulating the actual in situ case. The results obtained will allow for a clearer understanding of the response of offshore systems under real-world conditions and guide related analysis and design approaches. While the literature is rich with studies that are aimed at quantifying the effect of temperature on the interface shear strength between solids and clays at relatively high pressures, there is

a pressing need for quantifying the effect in the low pressure range for applications involving offshore pipelines. In the chapter that follows, a literature review is presented covering the description of the testing setups and testing methodologies of interface behaviour at low confinement stresses along with the effect of temperature on the pipe-soil interface resistance.

CHAPTER II

REVIEW OF LITERATURE

A. Lab Element Testing of Interface Resistance at Low Confinement Stresses

Experimental studies on soil-pipeline interface behavior have recently been a subject of interest to researchers. The usual range of normal stresses that geotechnical applications experience is much larger than the range of normal stresses acting at the pipe-soil interface in offshore applications. Conventional devices used are not designed to model such small stress ranges. This lead to the development of new devices targeting low normal stresses. Other efforts were made to account for low stress ranges by modifying conventional devices at hand. (Westgate et al., 2018a) summarized all the available element testing devices showing the advantages and limitations of each **Table 1**.

The modified direct shear is the most common device used for measuring the soil/structure interface. (Westgate et al., 2018a) suggested a site-specific test program using the interface direct shear device to get initial reliable estimates of the axial pipe-soil interaction parameters. The program was based on data from more than 200 tests performed on several soft clays and pipeline coatings. They concluded that the modified interface direct shear device can provide accurate measurements of the axial interface resistance resembling the actual pipeline in-situ response. However, the mechanical friction of the set up itself has large impact at low effective stress and therefore must be accounted for. Other limitations of this device include its relatively short horizontal displacement and its inability to measure pore pressures developed in the soil.

Table 1 Element testing devices for measuring interface shear resistance (Westgate et al., 2018a)

Device	Example Image	Mechanical Description	Advantages	Limitations	References
Direct interface shear box (ISB)		Interface surface sliding below a fixed square or circular specimen	Controlled displacement rate; simple apparatus; wide experience.	Short horizontal displacement range; no pore pressure measurement; potential box friction errors	Potyondy 1961, Tsubakihara and Kishida 1993
Ring shear		Interface surface rotating under fixed annular specimen	Unlimited displacement achievable	Slight variation in strain rate radially across specimen; no pore pressure measurement	Bishop et al. 1971, Bromhead 1979, Yoshimi and Kishida 1981, Stark and Eid 1993
Cam-shear		Circular specimen sliding above a fixed interface surface (similar to ISB)	Controlled displacement rate; simple apparatus	Short horizontal displacement range; no pore pressure measurement	Bolton et al. 2007, Kuo 2011, Ganesan et al. 2013
Tilt table		Thin specimen sliding along titled interface surface	Simple apparatus, machine friction eliminated	Uncontrolled displacement rate; no pore pressure measurement; cyclic capability depends on set-up.	Pedersen et al. 2003, Najjar et al. 2003, Najjar et al. 2007
Cam-Tor		Circular interface rotating under fixed circular specimen	Less machine friction than ring shear and smaller specimen (can use intact samples); globally undrained testing possible (membrane surrounds sample); unlimited displacement achievable	Significant variation in strain rate radially across specimen	Kuo et al. 2015, De Brier et al. 2016

B. Thermal Effect on Interface Resistance

In recent decades, researchers focused on studying the effect of temperature on the interface resistance because of the increase in applications that involve subjecting geotechnical structures to high temperatures. Energy foundation applications include structural foundations that enable the exchange of heat with the surrounding soil. The increase in demand for such geothermal structures has lead researchers to further study the possible effect of temperature change on the soil surrounding the foundation as well as its effect on the deep foundation/soil interface. **Table 2** summarizes many of the studies focusing on this field of study.

Table 2 Summary of published experimental studies for interface testing in geothermal foundations

Reference	Temperature Studied (°C)	Normal Stress (kPa)	Soil Type	Soil Atterberg Limits	Shearing Rate (mm/min)	Interface Type	Interface Roughness (mm)	Results (as temperature \nearrow)	
(Di Donna et al., 2016)	Ranging between 20 and 60	50, 100, and 150 kPa	Bernasconi grey quartz sand.	NA	0.27	Concrete-Smooth	0.002	No effect	
						Concrete-Medium	0.12		
						Concrete-High	0.2		
			Illite clay	LL (%) 53.4 PL (%) 30.0 PI (%) 23.4	0.006	Concrete-Medium	0.5	\nearrow in strength \searrow in interface friction angle	
						Concrete-High	30	\nearrow of adhesion between the two tested materials	
(Yavari et al., 2016)	5°C, 20°C and 40°C	5 kPa to 80 kPa	Fontainebleau sand	NA	0.014	Concrete	0.7	effect on the friction angle and cohesion is quite small and therefore insignificant in this temperature range	
			kaolin clay	LL (%) 57 PL (%) 33 PI (%) 24					
(Yazdani et al., 2019)	cycled between 24°C and 34°C	150 kPa, 225 kPa and 300 kPa	kaolin clay	LL (%) 45 PL (%) 25 PI (%) 20	0.005	Concrete	Range: 0.88 and 5.38	NC: \nearrow in shear strength And a contractive volumetric behavior	OCR: \searrow in shear strength And no change in volumetric behavior
(Xiao et al., 2017)	4.5, 22.5, and 42.5 °C	27.6, 41.4, and 100	sandy silty clay (CL-ML)	LL (%) 28 PL (%) 22 PI (%) 6	3	Concrete	NA	Monotonic heating: \searrow of adhesion No effect on friction angle	Cyclic heating: \nearrow of adhesion \nearrow in friction angle

Reference	Temperature Studied (°C)	Normal Stress (kPa)	Soil Type	Soil Atterberg Limits	Shearing Rate (mm/min)	Interface Type	Interface Roughness (mm)	Results (as temperature \nearrow)
(C. Li et al., 2019)	2, 15, and 38 °C	50, 100, 200, and 400 kPa	Red clay	LL (%) 27.6 PL (%) 11.1 PI (%) 16.5	ranging from 0 to 2.40	porous stone disc	0.03392	Effect is negligible
(Wang et al., 2018)	8, 24, and 60 °C	50, 100, and 150 kPa	Quartz sand	NA	0.25	Concrete-Smooth	NA	No significant effect
			Red silty clay	LL (%) 49.5 PL (%) 22.6 PI (%) 26.9	0.006	Concrete	0.25	Both c (the adhesion strength) and δ (the interface friction angle) report considerable changes (\nearrow)
(Hanson et al., 2015)	2, 20, and 40 °C	50, 100, and 150 kPa	medium well-graded sand	NA	1	Steel	ranges between 0.615 and 19.352	Interface friction angle decreased slightly with temperature
(Maghsoodi et al., 2019)	5, 22, and 60 °C	100 and 300 kPa	kaolin clay	LL (%) 57 PL (%) 33 PI (%) 24	0.006	Stainless steel plate	NA	Positive impact on the shear strength of the interface in normally consolidated kaolin clay

(Di Donna et al., 2016) investigated the response of the pile–soil interface at temperatures ranging between 20 °C and 60 °C using a direct shear device developed and calibrated for nonisothermal soil–structure interface testing (**Figure 1**). They tested for different concrete roughness values using both monotonic and cyclic stress paths.

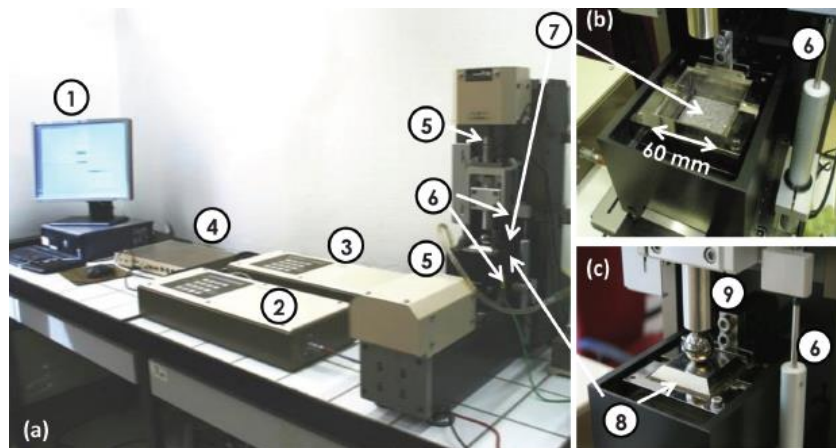


Figure 1 GDS Direct Shear device (Di Donna et al., 2016) - 1, GDSLAB software control, 2, normal actuator, 3, horizontal actuator, 4, LVDTs, acquisition pad, 5, load cells, 6, LVDTs, 7, specimen placement, 8, top cap, and 9, axial piston

Results showed that the sand–concrete interface behaviour is not affected by the temperature changes, while the response of the clay–concrete interface shows an increase of strength, a slight decrease in interface friction angle, and an increase of the adhesion with increasing temperature (**Figure 2**). The authors related these results to the thermal consolidation of clay, which results in an increase of the contact surface between the two materials.

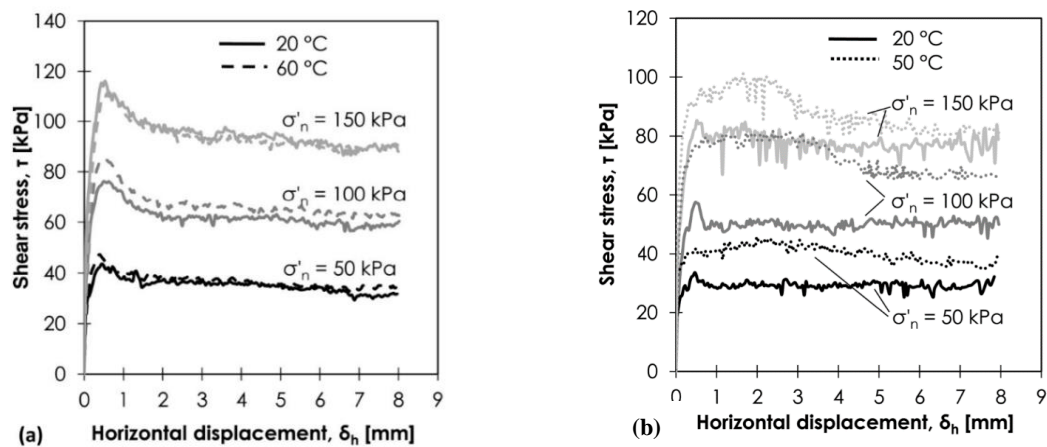


Figure 2 Effect of temperature on shear strength of (a) sand-concrete interface and (b) clay-concrete interface (Di Donna et al., 2016)

(Yavari et al., 2016) tested the shear behaviour of sand, clay, and soil/concrete interface through direct shear tests (**Figure 3**) at temperatures of 5°C, 20°C, and 40°C. Their results showed a softening behavior after the peak for the clay/concrete interface and a hardening behavior for sand and clay. The results of the effect of temperature on the shear strength parameters (friction angle and cohesion) is shown in (**Figure 4**). They concluded that the effect of temperature on the friction angle and cohesion is quite small and therefore insignificant in this temperature range (5°C -40°C). They also compared their results with other studies to prove that friction angle is not affected by temperature increase.

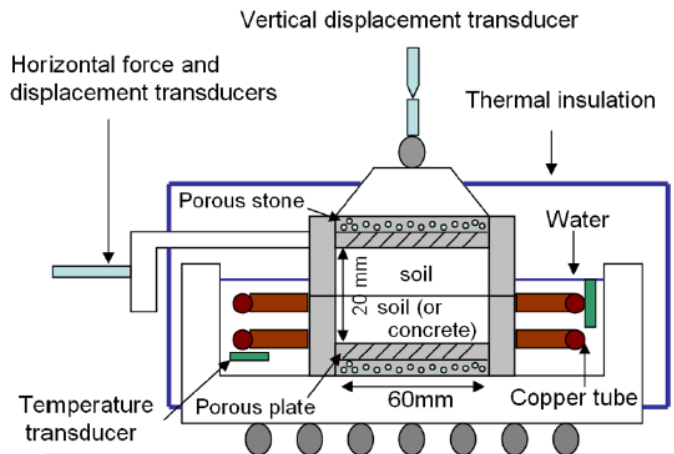


Figure 3 Direct shear apparatus with temperature control system (Yavari et al., 2016)

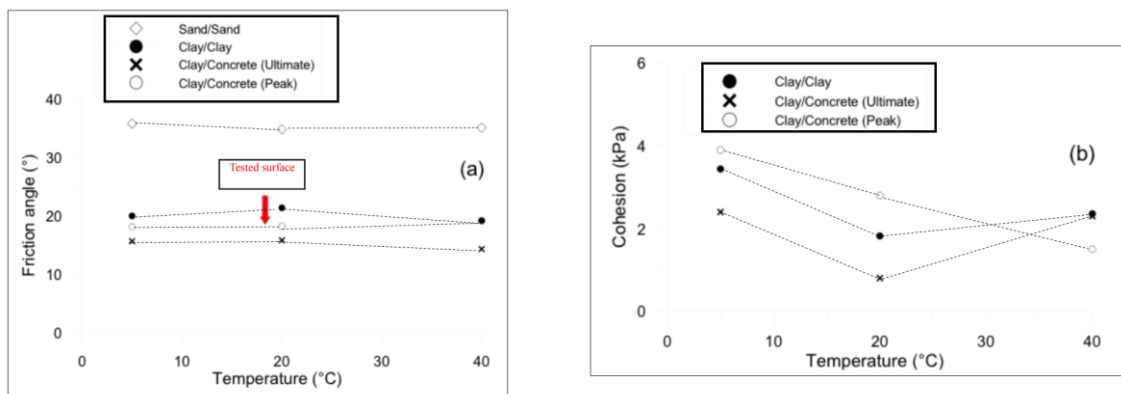


Figure 4 Effect of temperature on (a) friction angle and (b) cohesion

(Wang et al., 2018) tested the behavior of the interfaces between soil (quartz sand and red clay) and concrete under the effect of temperature change (**Figure 5**). Their results showed no significant effect on sand-concrete shear strength therefore similar to results of (Di Donna et al., 2016). On the other hand, considerable effect of temperature change on clay-concrete interface shear parameters was indicated. (**Figure 6**) shows these results clearly. As temperature increases, both c (the adhesion strength) and δ (the interface friction angle) report considerable changes.

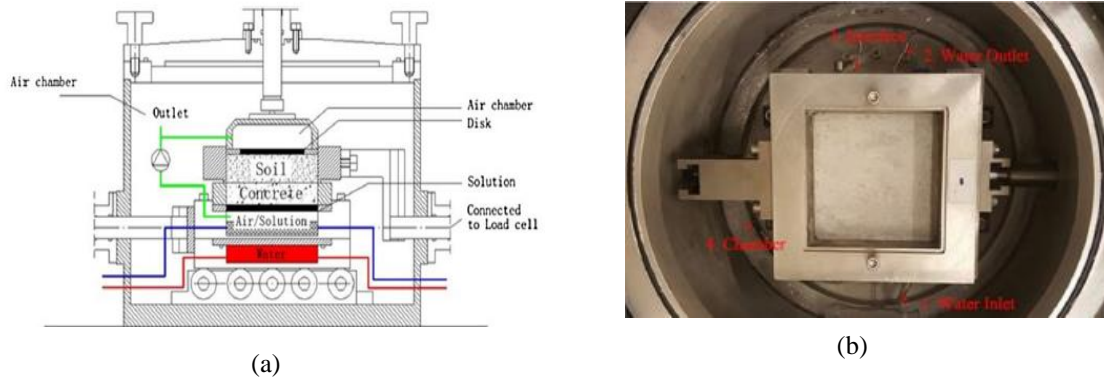


Figure 5 (a) Schematic diagram of new Direct Shear apparatus and (b) temperature monitoring sensors (Wang et al., 2018)

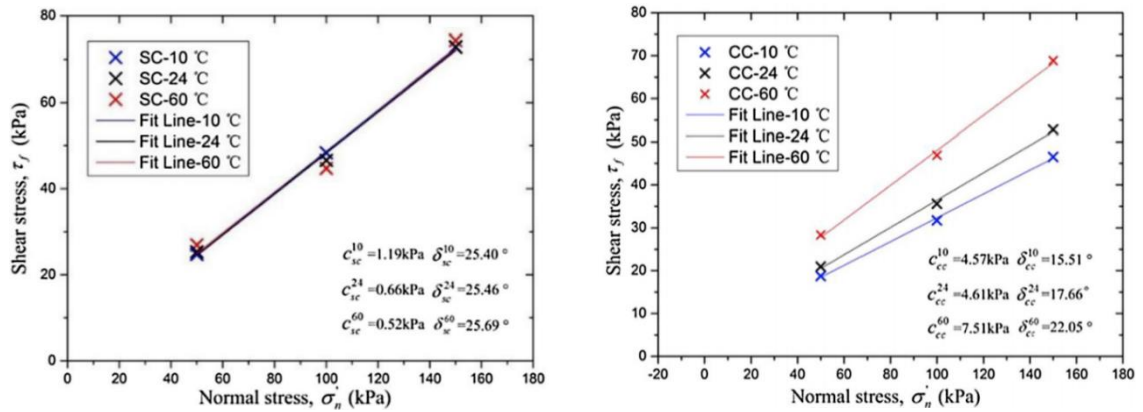


Figure 6 Impacts of thermal loads in the (a) sand-concrete and (b) clay-concrete interface tests on the net normal stress in relation to shear strength

Given the contradictory results reported in (Di Donna et al., 2016), (Yavari et al., 2016), and (Wang et al., 2018) in terms of the effect of temperature on the shear strength parameters for clay/concrete interface, more studies were later conducted, with particular focus on cyclic thermal loading (Xiao et al., 2017; Yazdani et al., 2019).

(Yazdani et al., 2019) studied the effect of temperature on soil/pile interface strength by applying non-cyclic and cyclic thermal loading under different stress states and histories (**Figure 7**). The temperature range tested was between 24°C and 34°C. They concluded that the effect of heating on the interface is governed by two factors: normal stress and overconsolidation ratio (OCR). Their results (**Figure 8**) showed that

heating generally improves the shearing resistance of normally consolidated (NC) clay/concrete interface with a contraction behavior observed during shearing. This improvement is manifested in cyclic thermal loading more than in elevated thermal loading and is more noticeable at higher normal stresses. As for OCR influence, both cyclic and non-cyclic thermal loading caused a reduction in shear strength proportional to the stress state history of the clay (OCR). With respect to volumetric behavior of interface during shearing, no thermally induced change was recorded as a function of OCR.

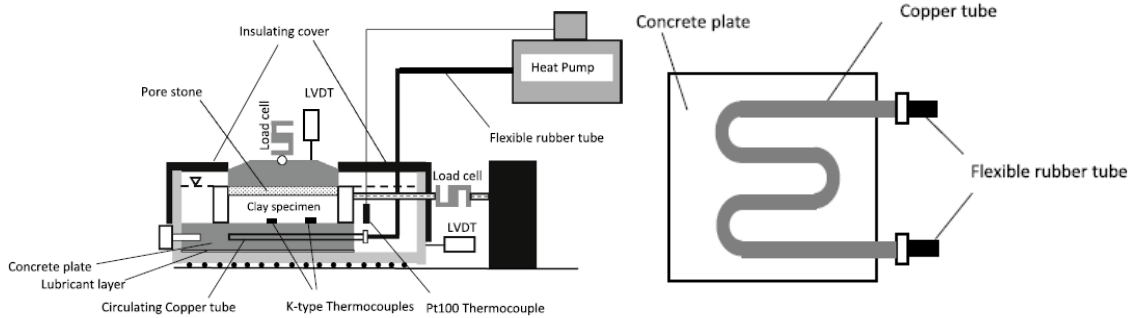


Figure 7 Schematic view of modified direct shear apparatus (b) Layout of the heating/cooling tubing in the concrete plate. (Yazdani et al., 2019)

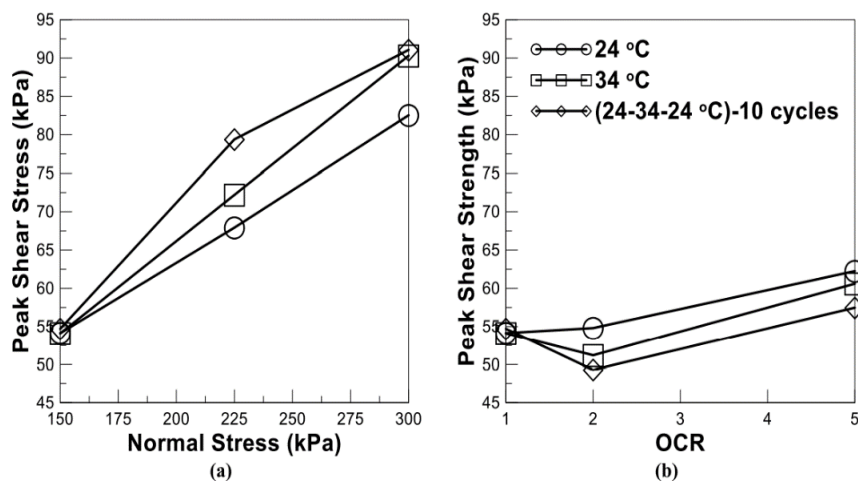


Figure 8 Effect of (a) interface normal stress, and (b) stress history of clay (OCR) on the thermo-mechanical response of interface (Yazdani et al., 2019)

(Xiao et al., 2017) investigated the effects of cyclic thermal loading on the shearing behavior of soil-structure interface using modified direct shear device (**Figure 9**). Tests were conducted with interface temperatures of 4.5, 22.5, and 42.5°C under cooling and heating conditions with temperature cycle (TC) numbers of 0.5 (monotonic cooling and heating) and 10.5 (cooling and heating cycles).

The reference test was at ambient temperature 22.5°C. Their study showed a 6 to 11% decrease in interface shear strength for TC=+0.5 (heating) and a slight increase (<3%) for TC=-0.5 (cooling). For thermal cycles TC=±10.5, cooling caused an increase by 10 to 20% and heating caused an increase by 14 to 23% of shear strength. Shear stress vs. displacement curves of soil-concrete interface under different normal stresses (27.6, 41.4, and 100 kPa) are illustrated in (**Figure 10**). The effect of temperature on interface friction angle and cohesion (adhesion) is shown in **Table 3**.

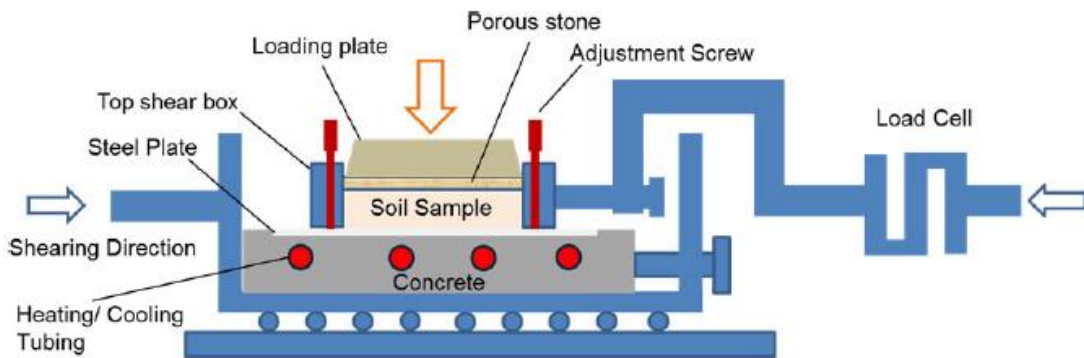


Figure 9 Modified Direct Shear test device (Xiao et al., 2017)

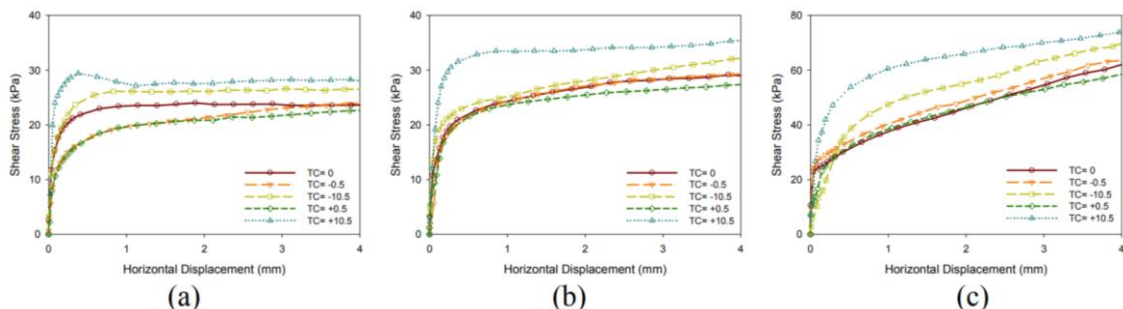


Figure 10 Shear stress-displacement curves of soil-concrete interface under different normal stresses (27.6, 41.4, and 100 kPa) (Xiao et al., 2017)

Table 3 Effect of temperature on interface shear parameters for sandy silty clay (Xiao et al., 2017)

condition		Cohesion (KPa)	Friction angel (°)	Moisture at the interface (%)
Ambient (22.5 °C)		8.3	28.1	18.6
Heating (22.5-42.5 °C)	normal	5.4	27.8	17.8
	10 cycles	11	32	16.4
Cooling (22.5-4.5 °C)	normal	8.9	27.8	18.7
	10 cycles	8.7	31.2	17.9

Cooling cycles had minor effects (8.3 to 8.7 kPa) on the adhesion of the soil-concrete interface while heating cycles showed an increase (8.3 to 11 kPa) in this parameter. Monotonic heating and cooling showed a decrease (8.3 to 5.4) and an increase (8.3 to 8.9) of adhesion, respectively. The friction angle increased by 3 to 4° upon both heating and cooling cycles. The authors linked this to moisture content change during the tests and soil particles rearrangement.

(C. Li et al., 2019) performed tests to evaluate the temperature effects on shear stress-strain behavior and shear strength parameters of red clay-geostructure interface under different normal stresses (50, 100, 200, and 400 kPa). A temperature-controlled direct shear apparatus (**Figure 11**) was used to perform tests at different temperatures (2, 15, 38 °C). They found that the effect of temperature on friction angle, cohesion of clay, and adhesion of clay-structure interfaces was negligible (**Figure 12**).

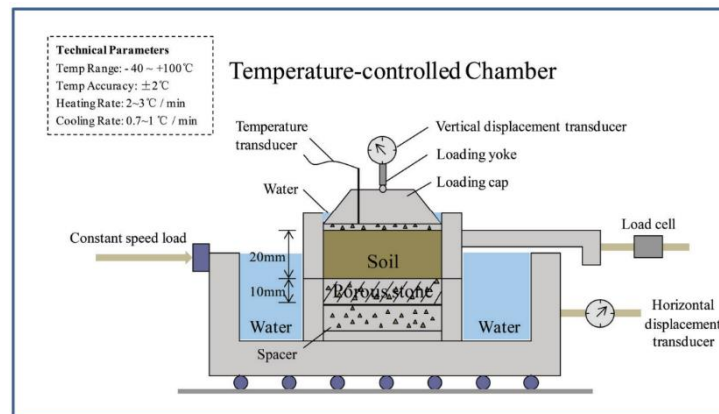


Figure 11 Direct shear apparatus in temperature-controlled chamber (C. Li et al., 2019)

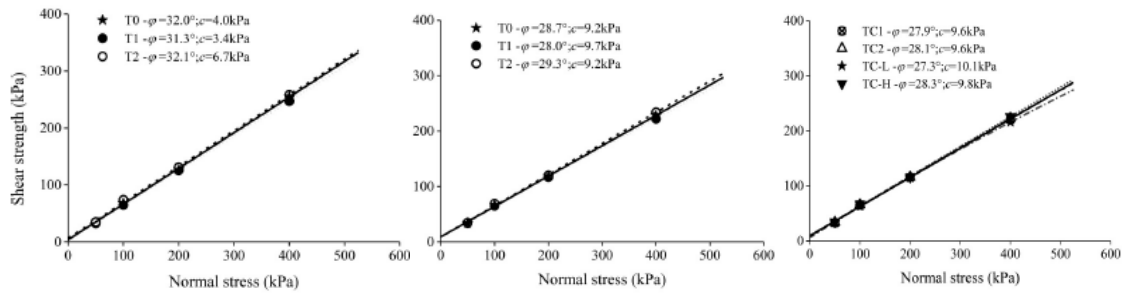


Figure 12 Failure envelopes of red clay–geostructure at different temperatures

(Maghsoodi et al., 2019) performed direct shear tests (**Figure 13**) on kaolin clay-stainless steel interfaces representing energy geo-structures to study the effects of temperature on their mechanical parameters. Constant Normal Load and Constant Normal Strain tests were done at temperatures of 5, 22, and 60°C taking into consideration the structure surface roughness. They concluded that temperature increase has a positive impact on the shear strength of the interface in normally consolidated kaolin clay. The results showed that the peak adhesion at the clay-structure interface increases from 12 to 18 kPa (**Figure 14**).

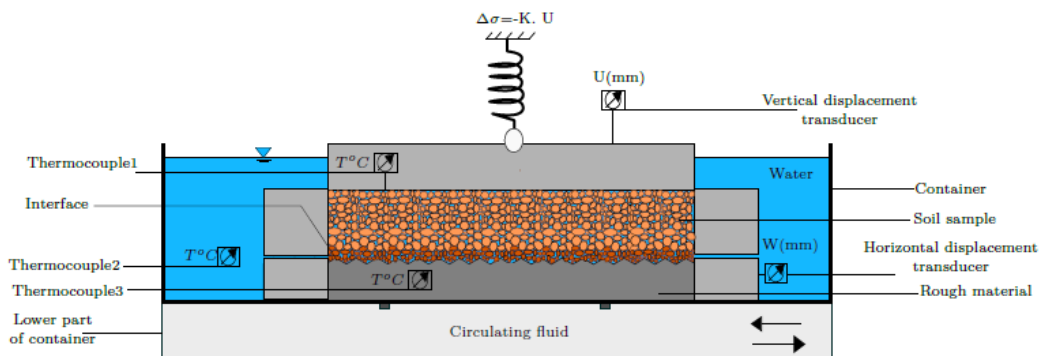


Figure 13 Experimental setup of the direct shear temperature-controlled device (Maghsoodi et al., 2019)

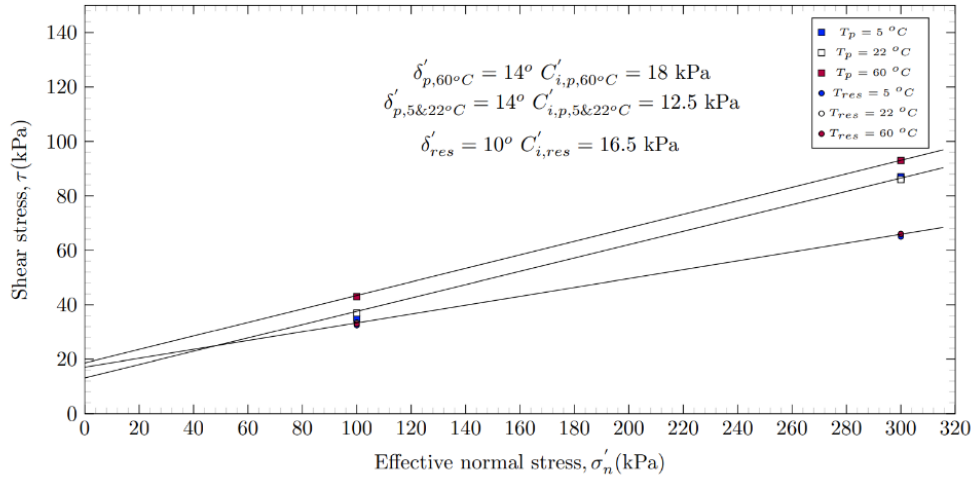


Figure 14 Shear stress vs. effective normal stress of CNL tests of clay-structure interface at different temperatures

Results from the literature indicate that the roughness of the interface material is a very important parameter which controls the soil-pipeline interface response. Potyondy (1961) first determined the magnitude of interface friction angle through a series of tests on soil-structure interfaces. He concluded that surface roughness significantly affects the friction angle and the adhesion of the interface. After that, (Uesugi & Krshida, 1987) performed a systematic study about the effect of roughness on the interface shearing resistance and defined it through the normalized roughness R_n , such that:

$$R_n = \frac{R_{max}}{D_{50}}$$

Where R_{max} is the maximum vertical distance between the highest and the lowest peaks of the structure surface in a gauge length L and D_{50} is the soil mean grain size.

Available research (Hu & Pu, 2004; Uesugi et al., 1989; Uesugi & Krshida, 1987) indicates that the critical roughness (R_{crit}) that distinguishes between rough and smooth interface response is defined in the range of 0.1-0.13, i.e. $R_n < R_{crit}$ indicates a smooth interface and $R_n > R_{crit}$ indicates a rough interface.

Various roughness parameters have been developed and used in the literature to characterize the roughness of a solid surface. Some utilize R_n , while others use R_{max} or R_a which is defined as the center line average roughness given by:

$$Ra = \left(\int_0^L |z(x)| dx \right) / L$$

Where $z(x)$ is the height of the profile from the mean line and L is the assessment length (Ward, 1982).

Interface roughness affects the shear strength and the vertical deformation of the soil–structure interface. (Hu & Pu, 2004) tested dense sand against a steel interface and their results (**Figure 15**) showed that the shear resistance is higher for rough interfaces. This finding confirmed results from many previous researches (Tsubakihara et al., 1993; Uesugi & Krshida, 1987). Similar results are reported for clay–solid interfaces. (Shakir & Zhu, 2009) performed interface simple shear experiments on compacted clay-concrete interfaces with different surface roughness and their study showed that the rough surface had higher interface shear strength (**Figure 16**). (Rouaiguia, 2010) performed interface direct shear tests on clays sheared against glass and sandstone rock, representing smooth and rough surfaces. His results showed that the smooth clay–glass interface exhibits lower strength values, which may be due to the different particle orientations along the interface zone caused by different roughness of the interfaces.

(Chen et al., 2015) also studied the effect of surface roughness on different types of red clay-concrete interfaces by performing large-scale direct shear tests. They concluded that the rougher interfaces still exhibit weaker shearing resistance than the clay, but stronger shearing resistance than the smooth interface (**Figure 17**).

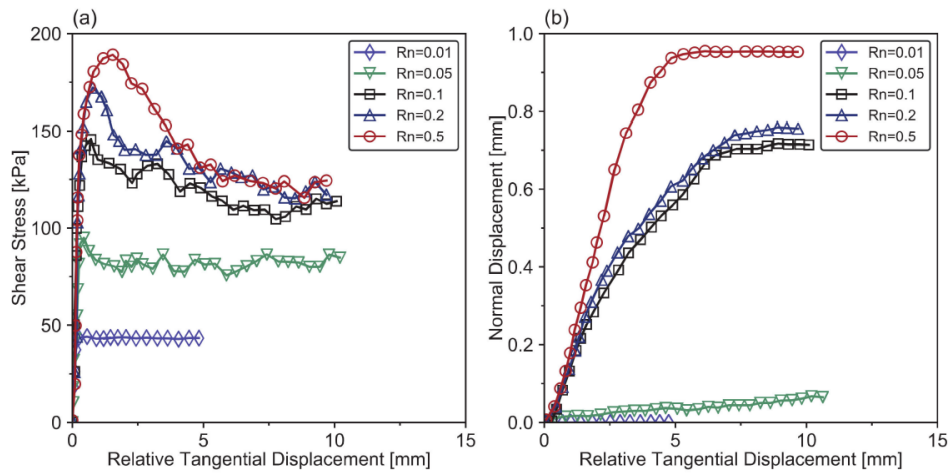


Figure 15 Effect of normalized roughness on sand-steel interface response under CNL conditions (a) shear strength and (b) vertical deformation, as a function of relative tangential displacement (Hu & Pu, 2004)

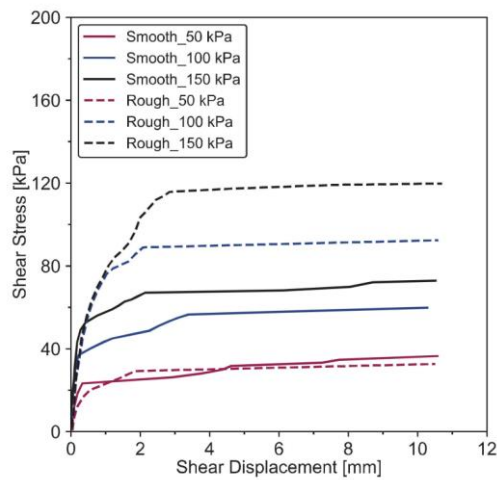


Figure 16 Shear stress vs. shear displacement of clay-concrete interface for different roughness (Shakir & Zhu, 2009)

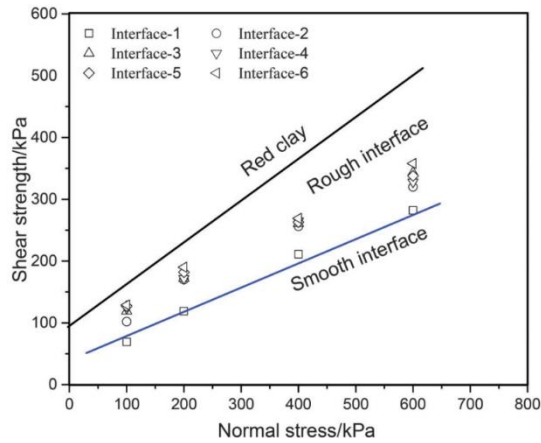


Figure 17 Mohr-Coulomb envelopes of clay-concrete interfaces (Chen et al., 2015)

(Tsubakihara et al., 1993) classified the interface behavior between cohesive soils and steel using three failure modes (**Figure 18**): full sliding at the interface (smooth), shear failure within the soil (rough), and the mixed behaviour where interface sliding and shear deformation of the soil specimen proceed simultaneously. (DeJong et al., 2003; Uesugi et al., 1988) confirmed this theory through particle image velocimetry at the interface. These results show that shearing deformation of the soil and the relative displacement between the two materials (sliding) govern the shearing response in clay-structure interface behavior despite the limited available results.

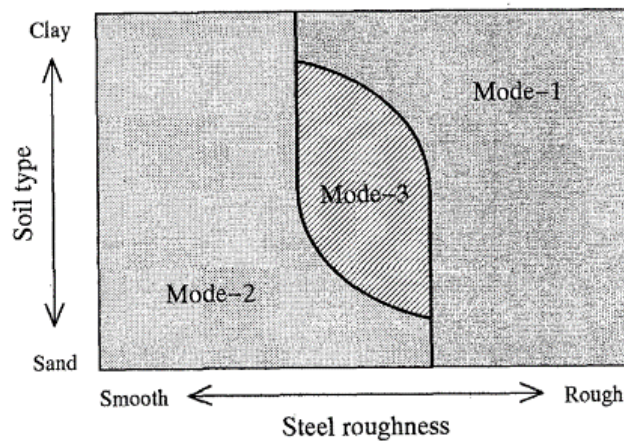


Figure 18 Classification of failure modes (Tsubakihara et al., 1993)

CHAPTER III

MATERIALS AND METHODS

The most common method for measuring the soil/structure interface strength is the Direct Shear Test. This test works to obtain the shear parameters under different working conditions in order to reveal the factors that influence the soil-structure interaction response. The solid material is placed in the bottom part of the shear box and the soil in the upper part.

Special attention is given to the description of the modified experimental device developed for this study. All the modifications made to adapt it to the interface testing at low confinement pressures and non-isothermal conditions are described as well as the mechanical and thermal calibration of its components.

A. Description of the Modified Direct Shear Apparatus

A modified-for purpose direct shear apparatus that allows for very low normal stresses, minimal system mechanical friction, and the control of interface temperatures is used to investigate the effects of temperature change on the soil-pipe interface properties (**Figure 19**). The measurement instruments were upgraded to guarantee high precision readings of the very low shear forces (Omega load cell capacity of 50 N and 0.05 N accuracy) and the vertical and horizontal displacements (LVDT with 0.001 mm accuracy). Vertical displacement, horizontal displacement, and shear force are continuously networked through a DAQ system to the computer. LabVIEW code was used to display the measurement onscreen in real time.

To reduce friction, many steps were taken. The steel shear box was replaced by a custom-fabricated Teflon box of lighter weight and a lower sliding resistance. The conventional loading method (lever arm and eccentricity) was improved by adding a

frictionless loading frame where dead weights are applied directly on top of the sample to ensure zero eccentricity and load uniformity.

In the modified direct shear test, the bottom half of the conventional shear box was developed using aluminum in order to withstand elevated temperatures. This part was fitted, in a certain configuration (**Figure 20**), with copper tubes of 3mm diameter connected to a heating circulator. Hot water from the circulator passes through the copper tubes in a closed loop system in order to raise and sustain the interface's temperature at the desired levels. The upper shear box remained the same, so the soil sample had a 60mm×60mm section with a height of 10mm.

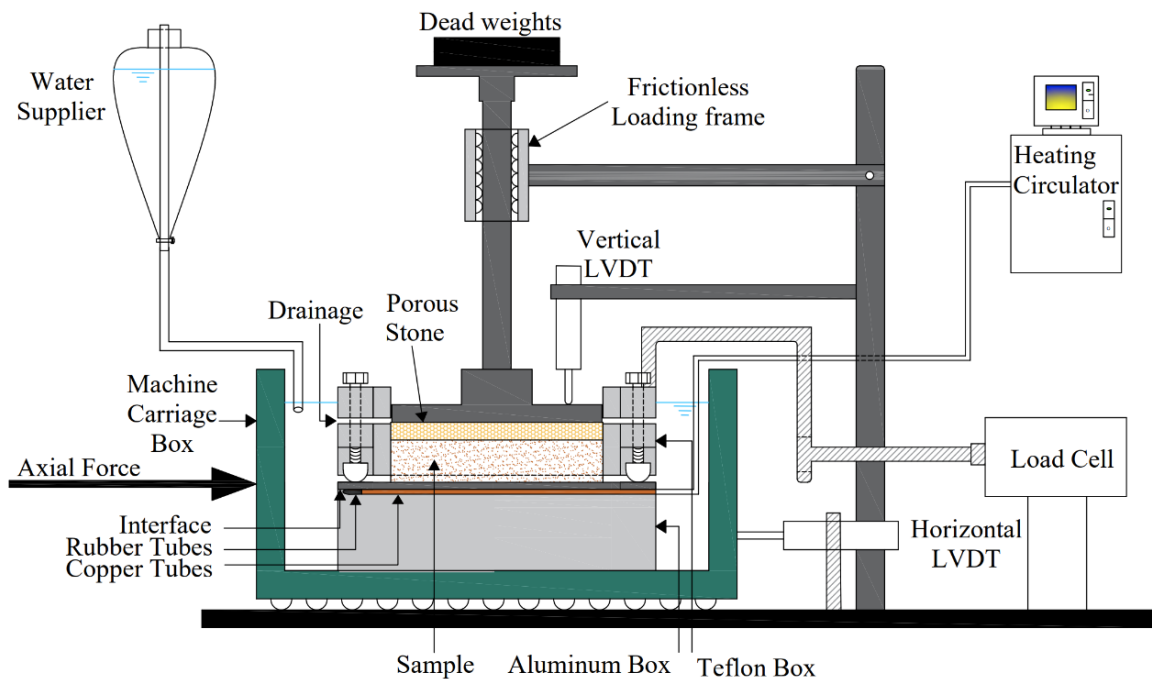


Figure 19 Modified direct shear setup

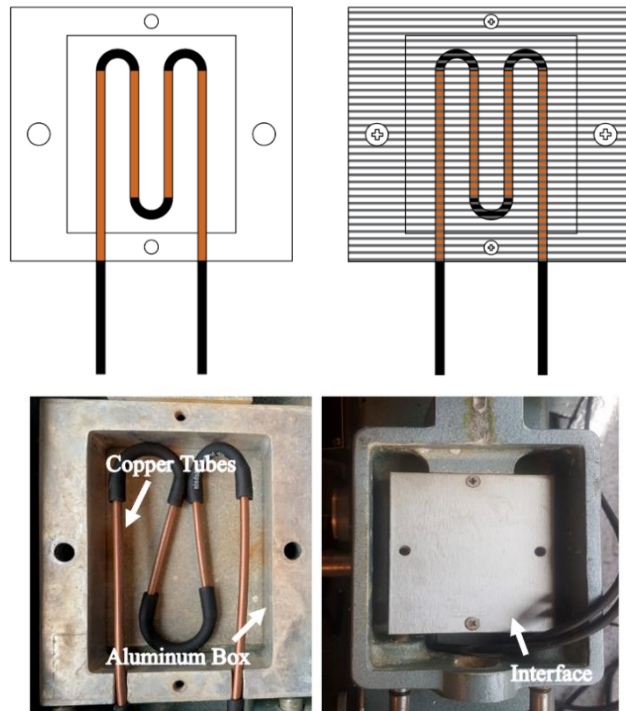


Figure 20 (a) Schematic drawing and (b) real image of copper tubes configuration in lower box

A water supplier (**Figure 21**) was utilized to account for the evaporation of water due to heating. This supplier releases a drop of water into the shear box every time the level of water lowers due to evaporation. In this way, the level of water in the shear box will remain constant throughout the test.



Figure 21 Water supplier

B. Materials

1. Soil

The soils used in the testing program are (1) a natural clay with low plasticity (LPC) and (2) a synthetic clay with high plasticity (HPC) (**Figure 22**), with specific gravities of 2.63 and 2.78, respectively. The LPC is a mix of 26% sand and 74% fines (**Figure 23a**). It has a liquid limit $LL=28.9\%$ and a relatively low plasticity index $PI=12.5\%$. The HPC is comprised of 100% fines with all particles passing sieve no. 200 (0.075mm) (**Figure 23b**), and having a liquid limit $LL=83\%$ and $PI=12.5\%$. LPC is classified as CL as per the Unified Soil Classification System USCS (ASTM D2487) and HPC as CH.



Figure 22 (a) Natural Clay with low plasticity (LPC) and (b) High Plasticity Clay (HPC)

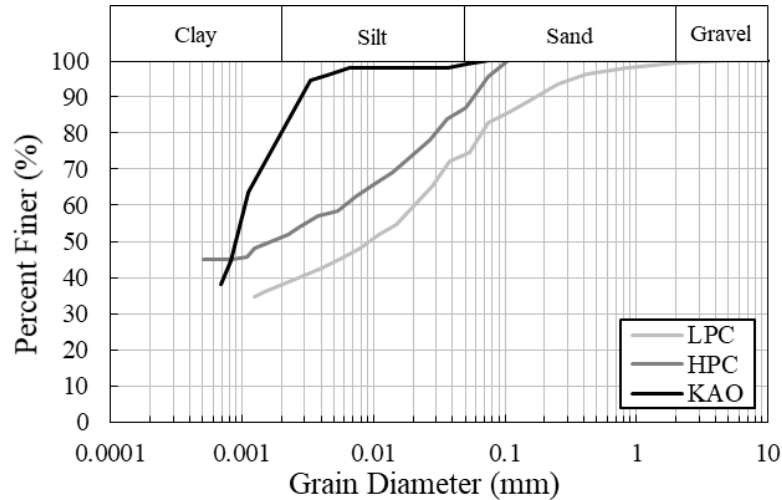


Figure 23 Grain-size distribution of (a) LPC and (b) HPC

The samples are prepared by mixing the tested soil at a water contents equal or greater than their liquid limits (water content of 30% and 100% for LPC and HPC respectively). Before testing, each reconstituted sample is left in a sealed cup after mixing for a duration of time to ensure homogeneity. The chosen duration is as per ASTM D3080 (**Table 4**). A minimum of 18 hours standing time for the LPC, and a minimum of 36 hours for the HPC is used. To start testing, the soil sample is remixed thoroughly then placed in the shear box. After that, a vertical load is applied and kept constant during the entire test (Constant Normal Load CNL test). To guarantee repeatability, the same quantity of soil is placed in the shear box for each of the normal stresses used in testing. Distilled water is added in the box to ensure saturated conditions.

Table 4 Minimum Standing Time for Samples prepared

Classification D2487	Minimum Standing Time, h
SW, SP	No requirement
M	3
SC, ML, CL	18
MH, CH	36

2. Interface Material

Two types of interface materials are used to represent offshore pipelines: stainless steel (**Figure 24**) and sandpaper (**Figure 25**), representing smooth and rough interfaces, respectively. The roughness of each interface was measured using a profilometer. The average roughness R_a of stainless steel is $0.284\mu\text{m}$ (**Figure 26**) and of sandpaper is $2.867\mu\text{m}$ (**Figure 27**). The sandpaper was glued to a stainless steel plate using epoxy. Sheets of size 100x90mm are prepared from both types and designed to be screwed to the lower aluminum shear box to guarantee a constant contact area between the two materials during shearing.

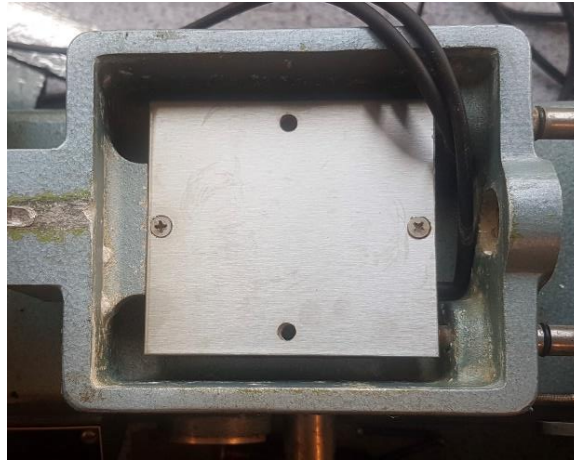


Figure 24 100x90mm Stainless steel sheets



Figure 25 100x90mm Sandpaper sheets

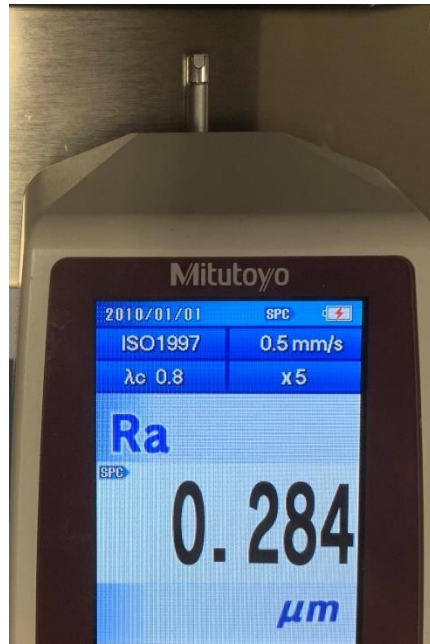
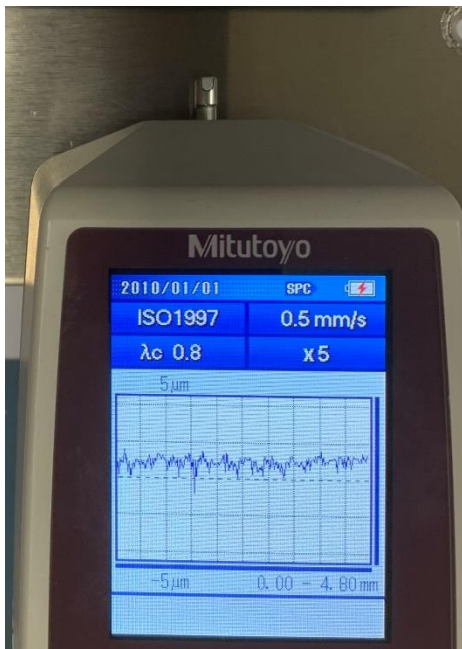


Figure 26 Profilometer readings for Stainless steel



Figure 27 Profilometer readings for Sandpaper

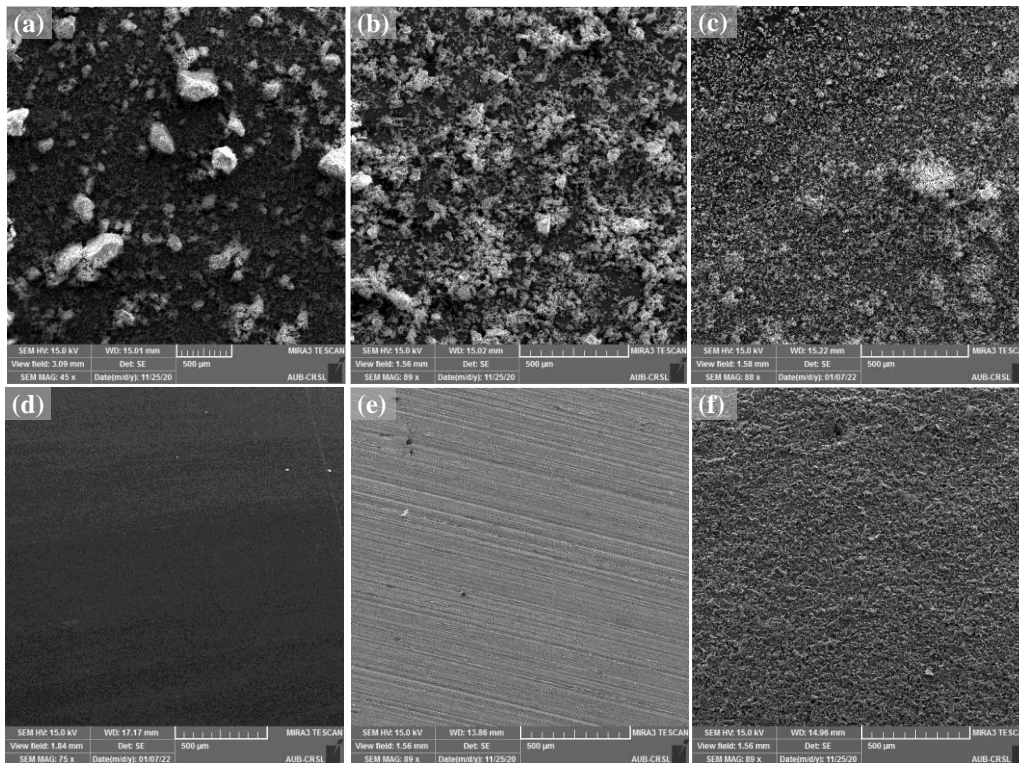


Figure 28 SEM images of (a) LPC, (b) HPC, (c) KAO, (d) Plexiglass, (e) Stainless Steel, and (f) Sandpaper

C. Test Procedure

After the soil samples were mixed at the desired water content they were placed in a sealed container to ensure homogeneity. Initially, the soil was placed in a 1cm thick square ring then placed in the upper part of the shear box. A moist filter paper and porous stone were placed above the sample followed by the loading frame and vertical LVDT. The consolidation phase was initiated by adding weights on top of the loading frame. The weights needed were chosen based on the applied normal stress.

After consolidation was completed, the heater circulator was turned on and hot water was pumped at a constant flow rate from the circulator through copper and rubber tubing into the shear box. After 2 hours, the maximum temperature of 60°C was reached, and heating was then maintained for 18 hours. To account for the evaporation

of water due to heating, the water supplier (**Figure 21**) was assembled to ensure that the water level in the shear box remained constant throughout the test.

During the shearing phase, the screws were loosened and a gap of around 0.7 mm was created between the interface and the upper box. Shearing tests were then performed at a slow rate of about 0.0024 mm/min to ensure drained conditions. Based on the consolidation curve, the time to failure to ensure drained loading conditions was computed using Equation (ASTM D 3080):

$$t_f = 50 \cdot t_{50}$$

Where t_f = total estimated elapsed time to failure in seconds and t_{50} = time required for the sample to achieve 50% consolidation. The shearing rate R_d is chosen to be $R_d = d_f/t_f$, where d_f is the estimated lateral displacement at the failure. This rate ensures that insignificant excess pore pressures are generated during shearing.

D. Setup Calibration

The vertical and horizontal friction of the setup should be measured and accounted for in the data analysis and determination of the interface shearing resistance. The setup was calibrated to take into account the friction of the device induced by both mechanical and thermal loading. A dummy sample made of steel was used to carry out the calibration tests and the same arrangement and procedure followed in real tests was used during calibration. Since different interface surfaces exhibit different levels of system friction, each structure interface was tested separately. The calibration tests were performed twice for each structure to check repeatability of the results.

The measured values of horizontal displacements and horizontal force (measured by load cell) were recorded in the calibration tests while heating the system to 60 degrees without a soil sample. **Figure 29a** shows that about 0.14 kPa of shear

resistance can be attributed to heating and friction of the testing system in the calibration test for stainless steel, while **Figure 29b** shows a higher shear stress 0.45 kPa in sandpaper tests. Corrections are thus needed to account for these additional stresses in the interface direct shear tests at elevated temperature. The vertical displacement was also recorded during the heating phase of calibration (**Figure 30**), and the results were used to correct the vertical displacement response of the real tests.

To verify “constant temperature” conditions, 3 thermocouples were placed on the interface and within the shear box (**Figure 31a**). The heating system was checked to verify a constant and homogeneous temperature in different locations of the shear box. **Figure 31b** shows that uniformity in temperature was attained and that the temperature remained constant after reaching its maximum value.

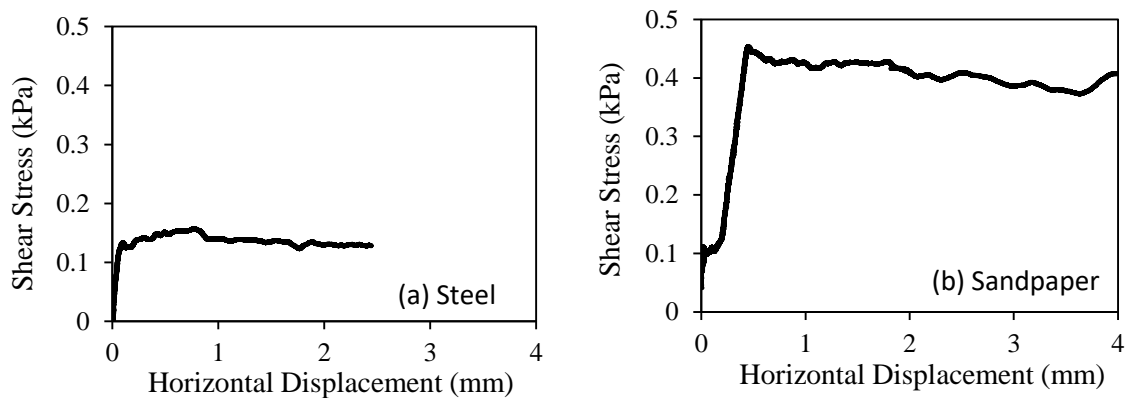


Figure 29 Friction and Temperature Effects on Shear Stresses for (a) Stainless Steel and (b) Sandpaper

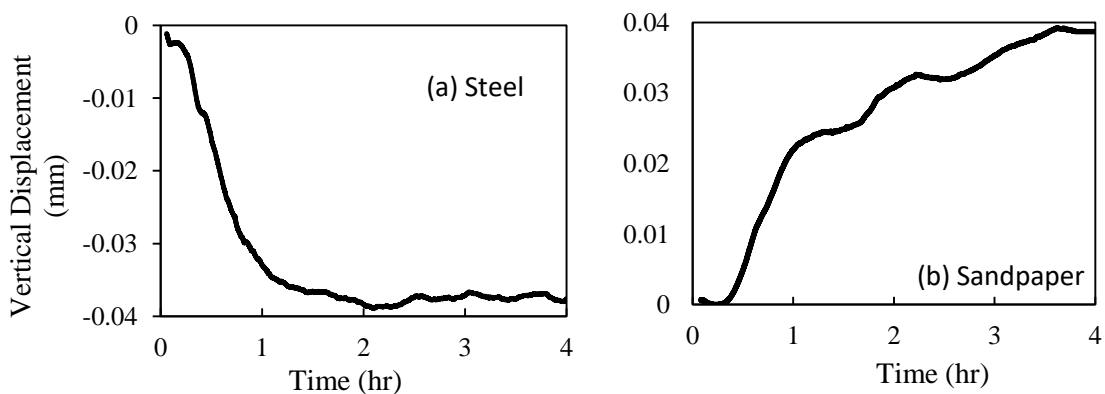


Figure 30 Vertical displacement due to elevated temperature

Calibration tests were also conducted to evaluate the effect of vertical friction along the inner sides of the shear box on the actual normal stress. **Table 5** shows the results of the calibration exercise which indicated differences of about 6% to 11% between the theoretical applied vertical stress on the specimen and the actual measured stress that is felt by the soil at the level of the shearing plane.

Table 5 Normal Stress Corrections due to Friction

Soil Type	Theoretical Normal Stress (kPa)	Vertical Friction (%)	Measured Normal Stress (kPa)
LPC	2.45	11	2.18
	4.26	9	3.87
	6.1	7	5.67
HPC	2.45	6	2.30
	4.26	6	4.00
	6.1	6	5.74

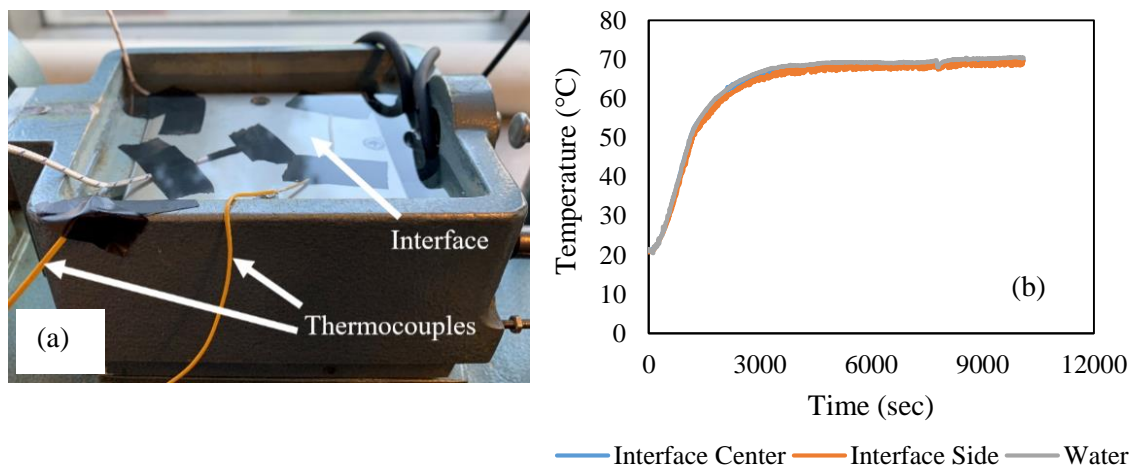


Figure 31 (a) Location of thermocouples (b) Temperature variation at different locations in shear box

CHAPTER IV

EXPERIMENTAL RESULTS

In order to evaluate the effect of temperature on the response of the clay-pipe interface, a series of experiments were performed at different vertical stress values (2.45kPa, 4.26kPa, and 6.1kPa) representing the stress normal to the pipeline's surface and at different temperatures. The results obtained are discussed separately for each phase of the experiment.

A. Consolidation Phase

The coefficient of consolidation (C_v) of LPC and HPC was estimated from the consolidation phase by considering one-way drainage conditions such that $C_v = 0.197 \frac{H^2}{t_{50}}$. With a sample thickness of 10mm, the average(C_v) is calculated to be approximately 2 $m^2/year$ for LPC and 0.21 $m^2/year$ for HPC. The consolidation graphs of the materials tested under the normal stresses 2.45, 4.26 and 6.1 kPa are shown in **(Figure 32)**.

It is clear from the graphs that at the same normal stress, HPC exhibits higher vertical deformation (settlement) than LPC. This is expected given the higher plasticity, void ratio, and water content of HPC compared to LPC. The range of vertical deformations for LPC is 0.25 to 0.45mm while that for HPC is 0.40 to 0.9mm, depending on the applied normal stress. It is also clear from **(Figure 32)** that the time required for consolidation to be completed under the applied normal stress is an order of magnitude greater in HPC compared to LPC, which is also expected given the lower permeability of the HPC.

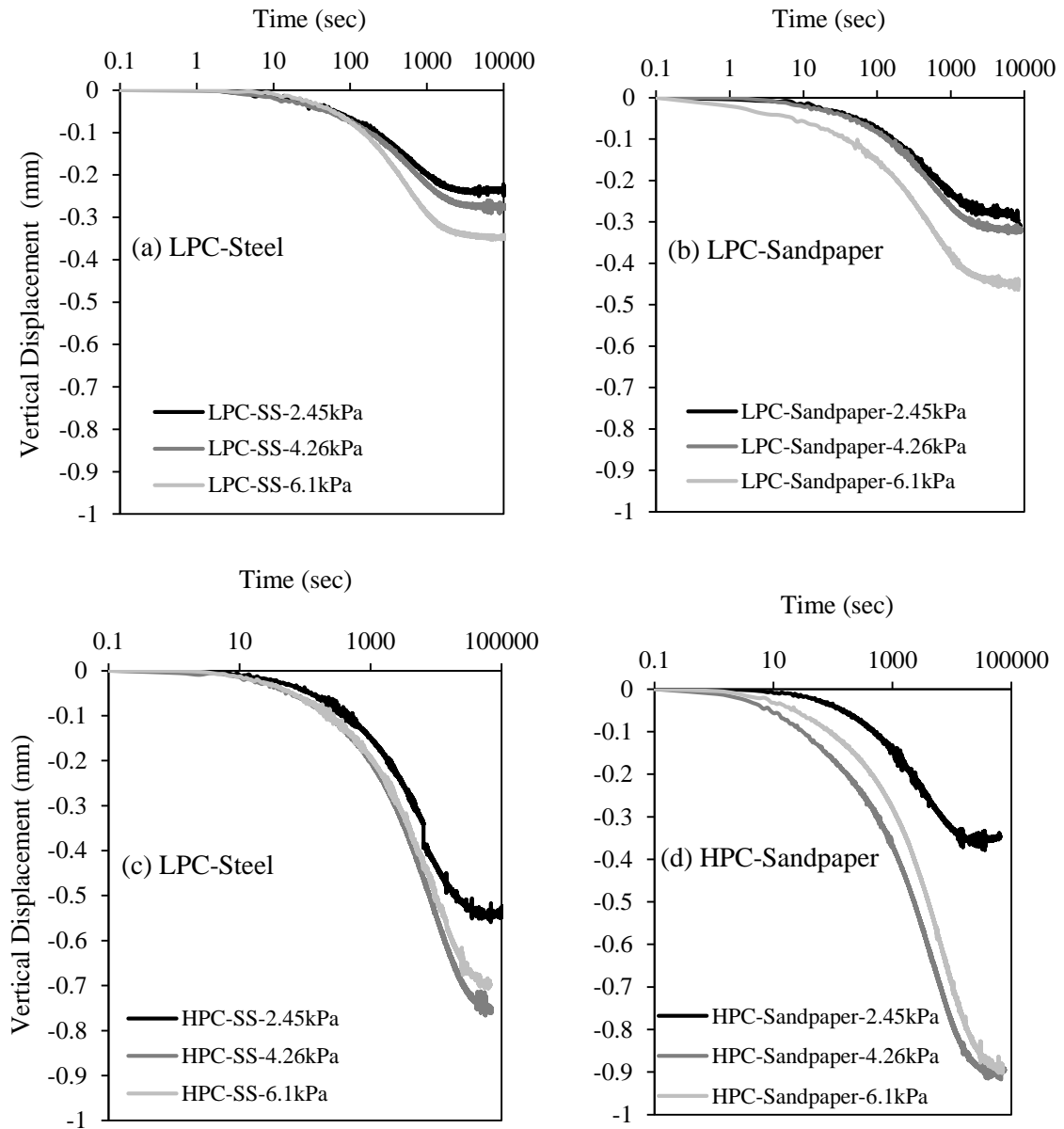


Figure 32 Consolidation curves at normal stresses of 2.45, 4.26, and 6.1 kPa

B. Heating Phase

Following the completion of primary consolidation under the applied normal stress, the interface was heated to raise the temperature from the reference of 22°C to 60°C.

Figure 33 shows the variation of the vertical displacement with time starting from the initiating of the heating phase. In addition to the tests that were conducted in the low pressure range (see test program in **Table 6**), a test was conducted using the LPC and

the stainless steel interface at a normal stress of 35kPa to represent the response in the normal pressure range and to identify the effect of normal stress on the vertical displacements due to increasing temperature prior to the shearing stage. The vertical deformation readings that are presented in (Figure 33) were corrected by subtracting from them the vertical deformations in the test setup (Figure 30).

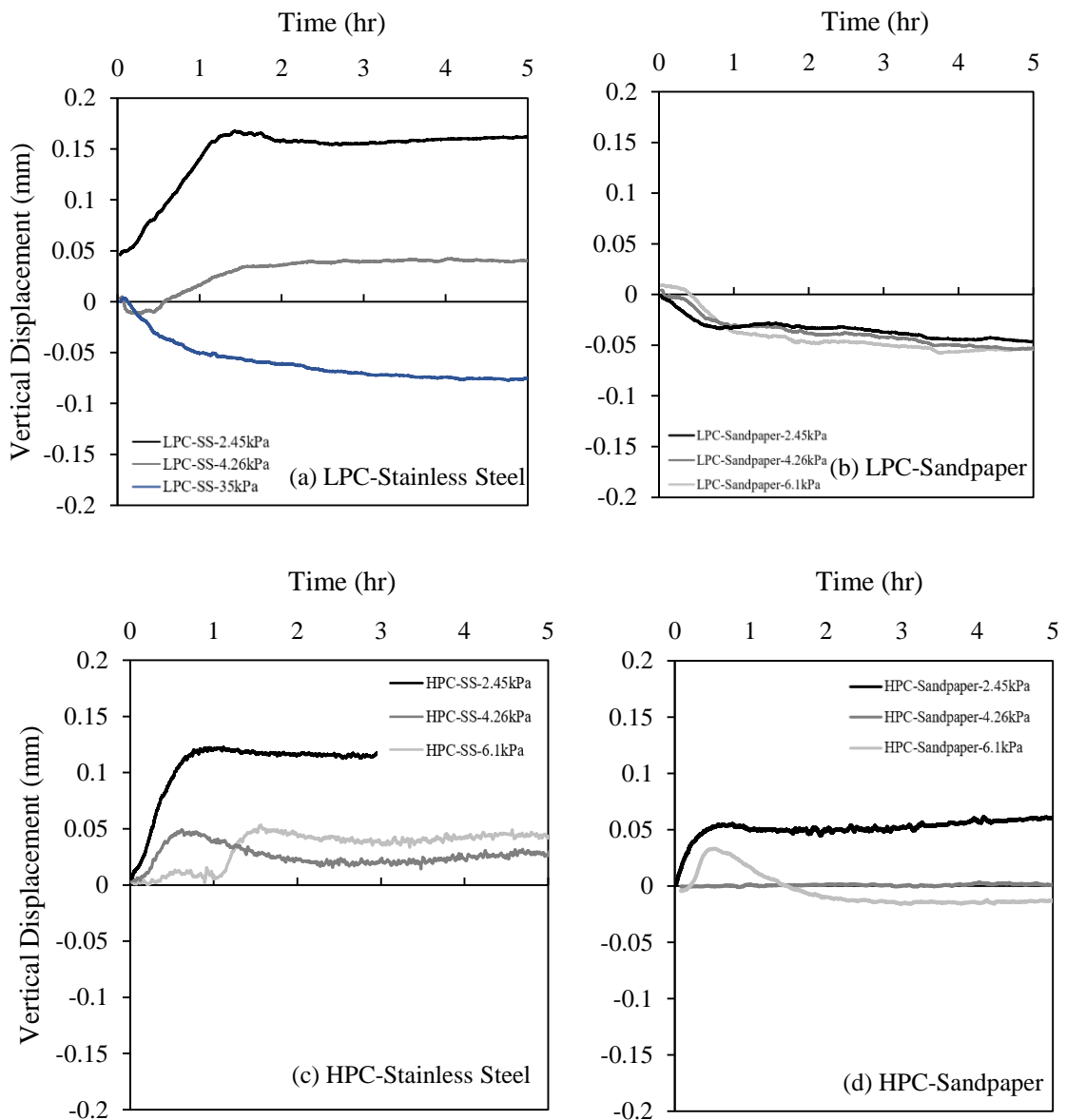


Figure 33 Vertical displacement vs. time from the start of heating

Results on **Figure 33a** and **33c** indicate that despite the completion of primary consolidation, upward vertical deformations (indicating swelling) in the order of 0.05mm to 0.17mm were observed for the Stainless Steel interface due to heating, irrespective of the soil type. The “swelling” response that was observed between LPC and stainless steel in the low pressure range (2.4 kPa to 6.1 kPa stress) was replaced by a contractive response when a relatively large normal stress of 35 kPa was applied. These results indicate that the expected contractive response that is typical of normally consolidated clay at elevated temperature may not be applicable in the very low pressure range where other factors may affect the response.

For the tests involving the rough sandpaper interface, results on **Figure 33b** show a slightly contractive response (vertical deformation ~ 0.05mm) due to elevated temperature under normal stresses between 2.45 kPa and 6.1 kPa. The HPC on the other hand exhibited a response ranging from slightly expansive (stress of 2.45 kPa) to slightly contractive at the larger stresses of 4.26 kPa and 6.1 kPa.

C. Shearing Phase

Table 6 summarizes the experimental testing program that was conducted in this study. **Figure 34** and **Figure 35** show the results of the interface tests conducted using the low plasticity clay (LPC) while **Figure 36** and **Figure 37** show the results of the tests conducted with the high plasticity clay. In all figures, results are presented for tests performed at temperatures of 22°C and 60°C to highlight the impact of elevated temperatures on the interface response. The response of clay-solid interfaces during the shearing phase focus on the shear stress versus horizontal displacement relationship and

on the drained peak and residual shear strengths as a function of the applied normal stress, clay type, and interface roughness.

Table 6 *Testing Program for Interface Direct Shear tests*

Test #	Soil Type	Interface Type	Effective Normal Stress (kPa)	Type of Loading
1	Low Plasticity Clay	Stainless Steel	2.45	Mechanical Loading (22°C)
2			4.26	Mechanical Loading (22°C)
3			6.1	Mechanical Loading (22°C)
4			2.45	Mechanical + Thermal (60°C)
5			4.26	Mechanical + Thermal (60°C)
6			6.1	Mechanical + Thermal (60°C)
7	Low Plasticity Clay	Sandpaper	2.45	Mechanical Loading (22°C)
8			4.26	Mechanical Loading (22°C)
9			6.1	Mechanical Loading (22°C)
10			2.45	Mechanical + Thermal (60°C)
11			4.26	Mechanical + Thermal (60°C)
12			6.1	Mechanical + Thermal (60°C)
13	High Plasticity Clay	Stainless Steel	2.45	Mechanical Loading (22°C)
14			4.26	Mechanical Loading (22°C)
15			6.1	Mechanical Loading (22°C)
16			2.45	Mechanical + Thermal (60°C)
17			4.26	Mechanical + Thermal (60°C)
18			6.1	Mechanical + Thermal (60°C)
19	High Plasticity Clay	Sandpaper	2.45	Mechanical Loading (22°C)
20			4.26	Mechanical Loading (22°C)
21			6.1	Mechanical Loading (22°C)
22			2.45	Mechanical + Thermal (60°C)
23			4.26	Mechanical + Thermal (60°C)
24			6.1	Mechanical + Thermal (60°C)

1. Effect of Temperature on Interface Response

a. Low Plasticity Clay (LPC)

Results of the interface direct shear tests involving LPC are presented in **Figure 34** and **35** for the clay-steel (smooth interface) and the clay-sandpaper (rough interface) tests. Results in **Figure 34** include the variation of the shear stress and vertical displacement with horizontal displacement while the results in **Figure 35** include the variation of the peak and residual failure envelopes, and variation of the secant friction

angle (peak and residual) with the logarithm of the normal stress. The peak and residual drained secant friction angles were estimated as the arc tangent of the ratio of the shear stress to the effective normal stress at peak and large displacements, respectively. An investigation of the stress–displacement curves leads to several observations.

First, the interface shear stress at a temperature of 22°C was observed to exhibit peaks at horizontal displacements in the order of 0.2 to 0.5 mm, in contrast to the elevated temperature tests (60°C) which exhibited a more ductile response with the peaks delayed to displacements of about 1 mm. After the peaks, the shear-stress versus displacement curves exhibited a softening response which ultimately stabilized at shear stresses corresponding to residual secant friction angles that were 3° to 5° smaller than the peak angles. The difference between peak and residual was not affected by the temperature conditions.

Second, for the LPC-steel interface tests, the peak and residual interface shear stresses were found to increase at 60°C. In contrast, the tests with the rough sandpaper interface showed that elevated temperature had a negative effect on the interface shear stresses, with clear reductions observed in both the peak and residual stresses at 60°C. For both smooth and rough interfaces, the effect of temperature on the observed shear stresses was found to be negligible at the highest normal stress of 6.1 kPa.

Third, the observed volumetric change as reflected through the vertical displacement during shear was found to be highly sensitive to the temperature conditions during the test. For the smooth interface, the LPC exhibited a compressive volumetric tendency during shear. This tendency clearly reduces at an elevated temperature of 60°C. An opposite volumetric response was observed with the rough interface, with clear signs of dilation during shear at ambient temperature and low

normal stresses. When the rough interface was heated to 60°C, results showed that the dilative volumetric changes were replaced by compressive volumetric changes at all normal stresses, indicating a significant roughness-dependent effect of temperature on the volumetric tendencies at the clay-solid interface during shearing.

Fourth, the drained Mohr-Coulomb failure envelopes were nonlinear, irrespective of temperature and roughness conditions. The nonlinearity is evidenced in the reduction in the drained residual secant friction angle as the normal stresses increased from 2.45 to 6.1 kPa. This nonlinearity was noted in previous studies (S. S. Najjar et al., 2007; Skempton, 1985; Stark & Eid, 1994) for clays at low stresses.

A comparison between the drained secant interface friction angles (peak and residual) at ambient and elevated temperatures indicates that for the case of the smooth interface, heating the interface to 60°C increased the peak friction angle by 5.5°, 2.5°, and 0.5° at normal stresses of 2.45 kPa, 4.26 kPa, and 6.1 kPa, respectively. The respective increase in the residual friction angle due to temperature was 4.5°, 1.5°, and 0°. Interestingly, heating the rough interface to 60°C decreased the peak friction angle by 4.5°, 1.5°, and 1.0° at normal stresses of 2.45 kPa, 4.26 kPa, and 6.1 kPa, respectively. The residual friction angles were also reduced by 4.5°, 1.0°, and 0°, respectively.

These reported changes in the peak and secant interface friction angles due to the effect of temperature are the first in the literature at low normal stresses. The main conclusion of the LPC tests is that the effect of heating the interface to 60°C is highly dependent on the roughness of the pipe (smooth versus rough) and the magnitude of the normal stress at the clay/soil interface. For very shallow pipe embedment (normal stress of about 2 kPa), significant differences in the interface response is observed at elevated

temperature. As the normal stress increases and approaches 6 kPa (pipe embedment increases), the effect of temperature on the interface response vanishes.

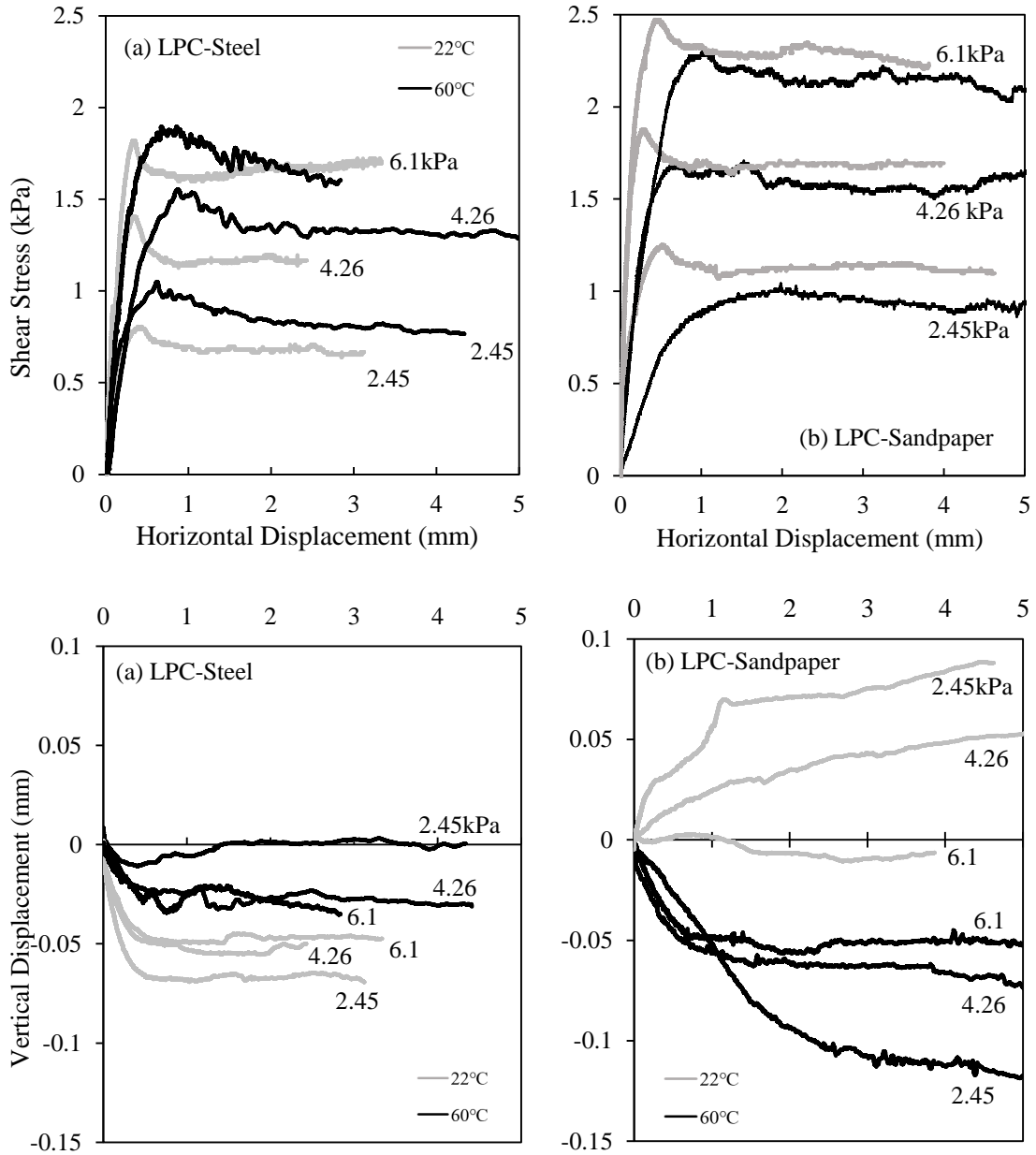


Figure 34 Interface response during direct shear testing at ambient temperature (22°C) and elevated temperature (60°C) for (a) LPC with Steel and (b) LPC with Sandpaper

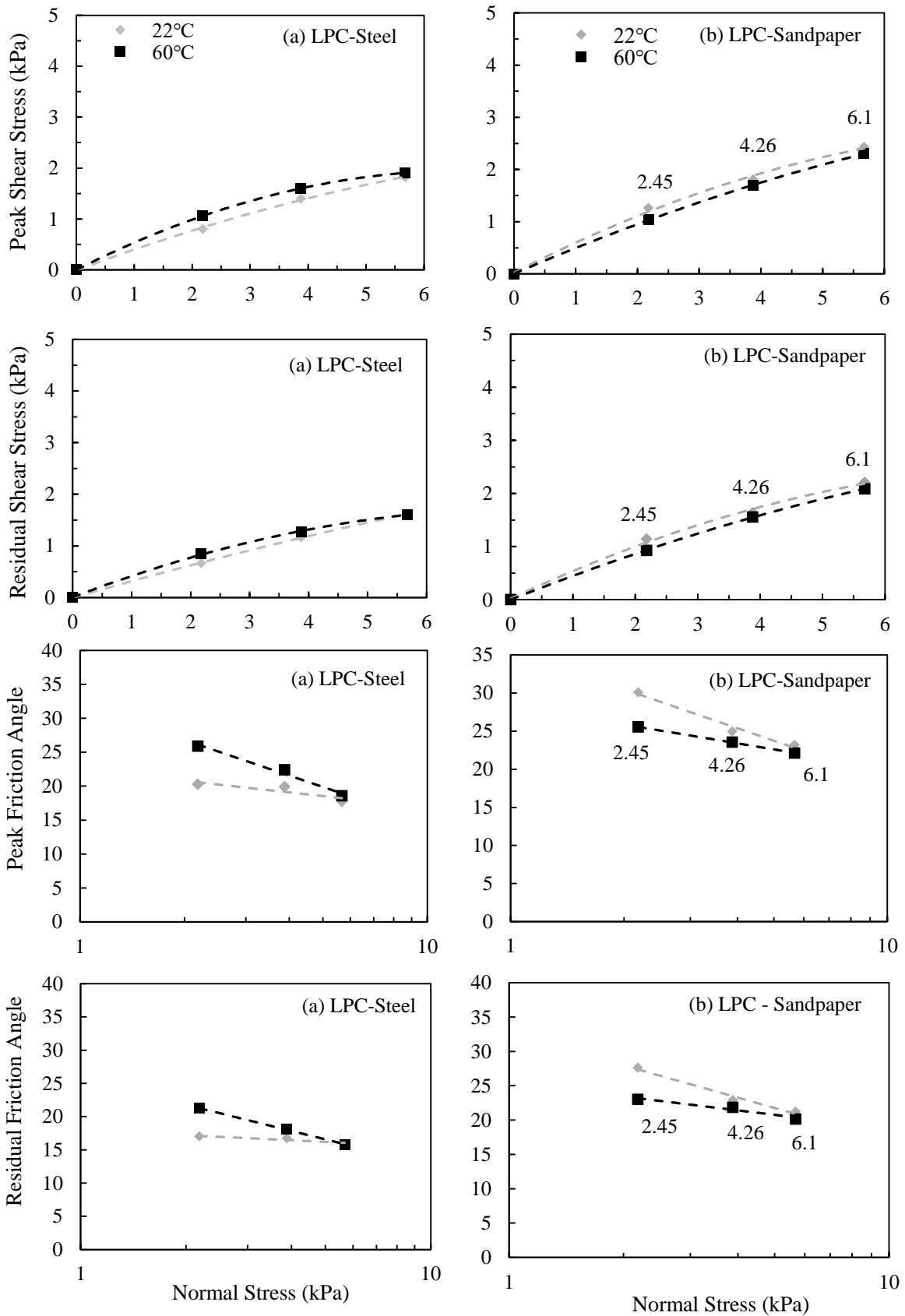


Figure 35 Variation of peak shear stress, residual shear stress, peak friction angle, and residual friction angle with normal stress for (a) LPC with Steel and (b) LPC with Sandpaper

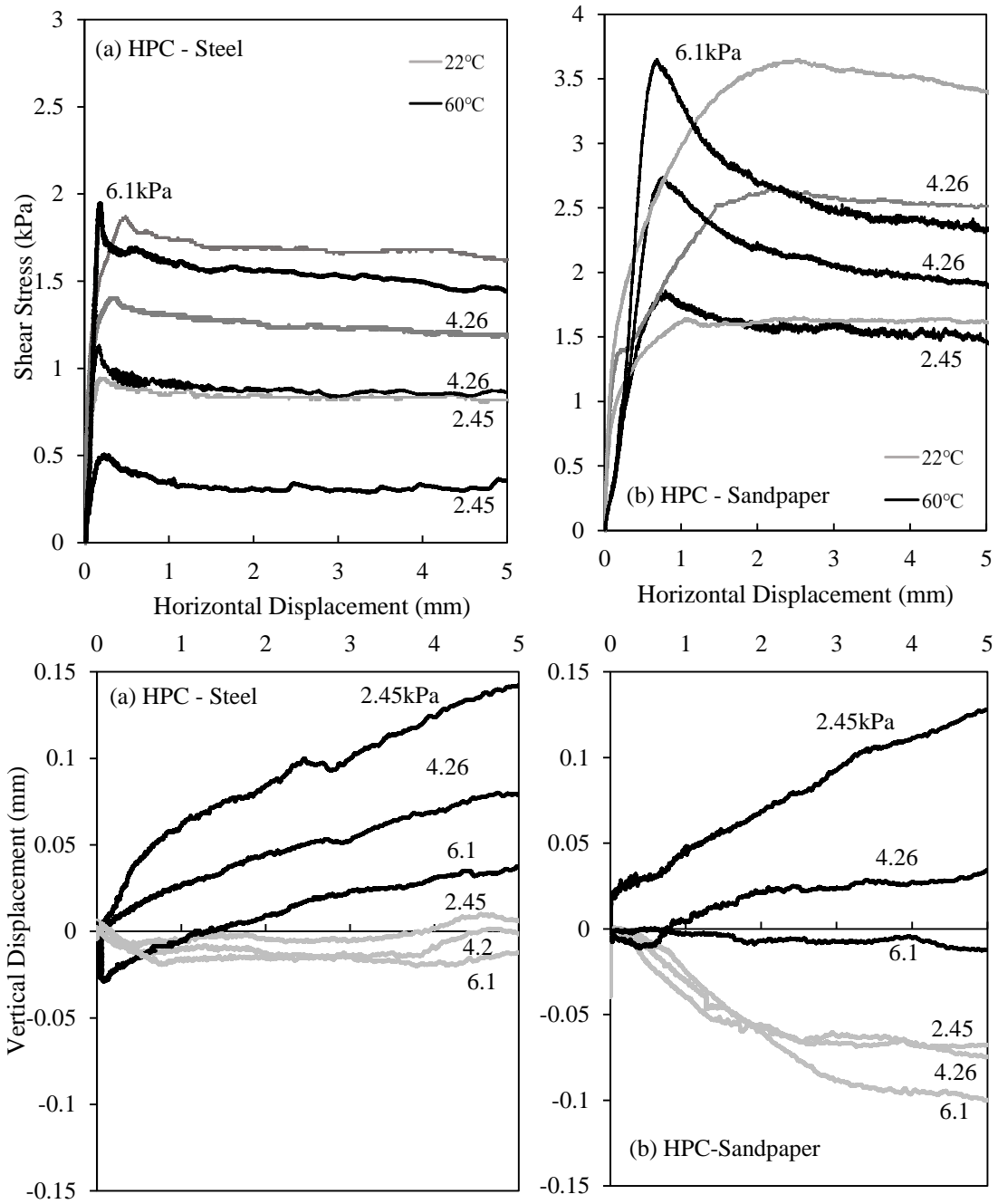


Figure 36 Interface response during direct shear testing at ambient temperature (22°C) and elevated temperature (60°C) (a) HPC with Steel and (b) HPC with Sandpaper

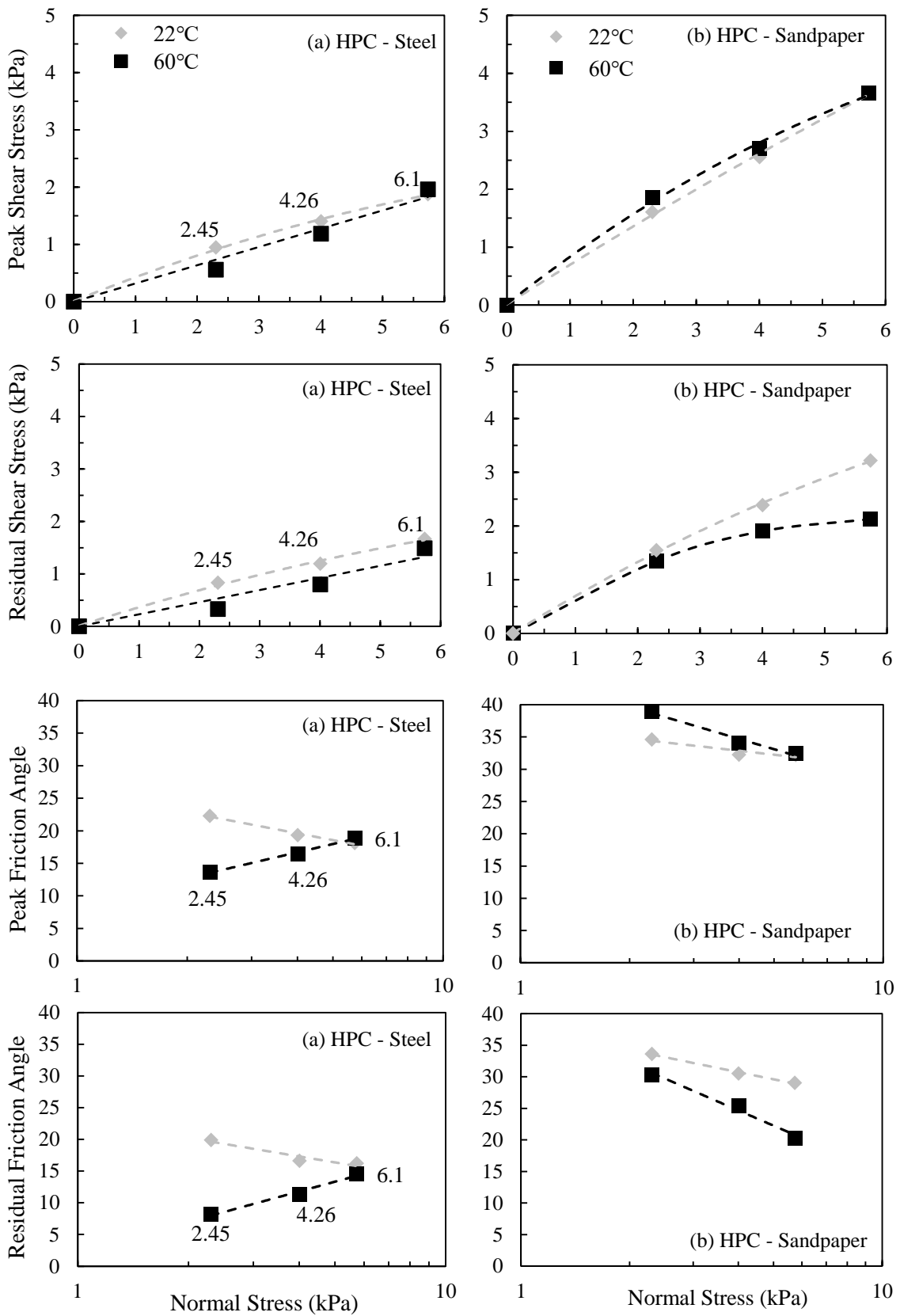


Figure 37 Variation of peak shear stress, residual shear stress, peak friction angle, and residual friction angle with normal stress for (a) HPC vs Steel and (b) HPC vs Sandpaper

b. High Plasticity Clay (HPC)

Results of the interface direct shear tests involving HPC are presented in **Figure 36** and **37** for the clay-steel (smooth interface) and the clay-sandpaper (rough interface) tests. Results in lead to the following main observations.

First, unlike the test with the LPC, the interface shear response for HPC at elevated temperature was more brittle compared to the test at ambient temperature with peaks in shear stress exhibited at relatively smaller horizontal displacements. At an elevated temperature of 60°C, the smooth steel interface exhibited peaks at displacements of 0.1mm (compared to 0.3mm at 22°C) while the rough sandpaper interface exhibited peaks at less than 1mm (compared to 1.5 to 2.5mm at 22°C). After the peaks, the tests at elevated temperature exhibited a brittle response that was characterized by significant softening to residual conditions. The brittle behavior was particularly observed in the rough interface tests at a temperature of 60°C and at the highest normal stress of 6.1 kPa.

Second, unlike the LPC tests which showed an increase in the peak and residual interface shear stresses at 60°C for the smooth interface, results for HPC showed a very marked decrease in peak and residual stresses for the smooth interface at elevated temperature, particularly at small normal stresses. The effect of temperature reduced dramatically at the highest normal stress of 6.1 kPa. On the other hand, results of the rough interface tests indicated that elevated temperature did not have a significant effect on the peak shear stress, but resulted in significant reductions in the residual stress at large deformations, particularly for the case involving normal stresses of 6.1 kPa.

Third, the observed volumetric change as reflected through the vertical displacement during shear indicated that increasing the temperature to 60°C in the case of HPC resulted in significant dilation at the interface during shearing for both stainless steel and sandpaper. As expected, the largest dilative volume changes were observed in tests conducted at the smallest normal stress of 2.45 kPa. The tendency for dilation due to elevated temperature was suppressed in the tests conducted at the highest normal stress of 6.1 kPa. It should be noted that HPC exhibited contractive vertical deformations for the tests conducted at ambient temperature for both the smooth and rough interfaces. Elevated temperatures replaced the contractive response of HPC during shearing to a highly dilative response that is indicative of “overconsolidated” clay behavior.

Fourth, the drained interface Mohr-Coulomb failure envelopes for HPC were found to be slightly nonlinear for tests conducted at ambient temperature as evidenced in the slight reduction in the drained residual secant friction angle as the normal stresses increased from 2.45 to 6.1 kPa. However, the failure envelopes at elevated temperature exhibited a complex behavior that was sensitive to the interface roughness, normal stress, and magnitude of shear deformations (peak versus residual).

For the smooth interface, reductions in the order of 8.7°, 3.0°, and 0° were observed in the peak friction angle due to elevated temperature for normal stresses of 2.45 kPa, 4.26 kPa, and 6.1 kPa, respectively. The respective decreases in the residual friction angle due to increase in temperature were 11.7°, 5.3°, and 1.6°. For the rough interface, heating to 60°C increased the peak friction angle by 4.3°, 1.8°, and 0° at normal stresses of 2.45 kPa, 4.26 kPa, and 6.1 kPa, respectively. Interestingly, the residual friction angles were reduced by 3.3°, 5.0°, and 9°, respectively due to heating.

These results confirm the observation that the interface response at elevated temperature is a complex phenomenon that is governed by multiple factors that include the plasticity and mineralogy of the clay, applied normal stress, pipe roughness, and magnitude of the applied displacement.

2. Effect of Pipe Roughness on the Mode of Failure

The surface roughness of a pipe is expected to have a significant effect on the interfacial shear strength and mode of failure, with the shear strength increasing with increased surface roughness level (Chen et al., 2015). This was clearly observed in our results for LPC and HPC where the shear strength of the rougher interface (sandpaper) is greater than that of the smooth interface (stainless steel) under the same conditions and normal stresses.

In general, the shear strength of a soil–structure interface is lower than or at most equal to the shear resistance of the soil. Correspondingly, many research results concluded that increasing the surface roughness will lead to an increase in interface shear strength and the behavior becomes closer to that of the soil (Chen et al., 2015; Shakir & Zhu, 2009; Tsubakihara et al., 1993). These observations were confirmed in this research even for tests that are conducted at elevated temperature.

Figure 38 and **39** show the failure mechanism that was observed at the interface for LPC and HPC at elevated temperature for the smooth and rough interfaces. Results indicate that a clean interface shear surface is observed when LPC and HPC were sheared against the smooth stainless steel interface with the mode of failure being controlled by slippage between steel and clay. On the other hand, observations of the mode of failure for the rough interface at elevated temperatures indicated that clay

particles adhered to the sandpaper during the shearing phase for both LPC and HPC, indicating a combined failure mechanism at the clay-interface.

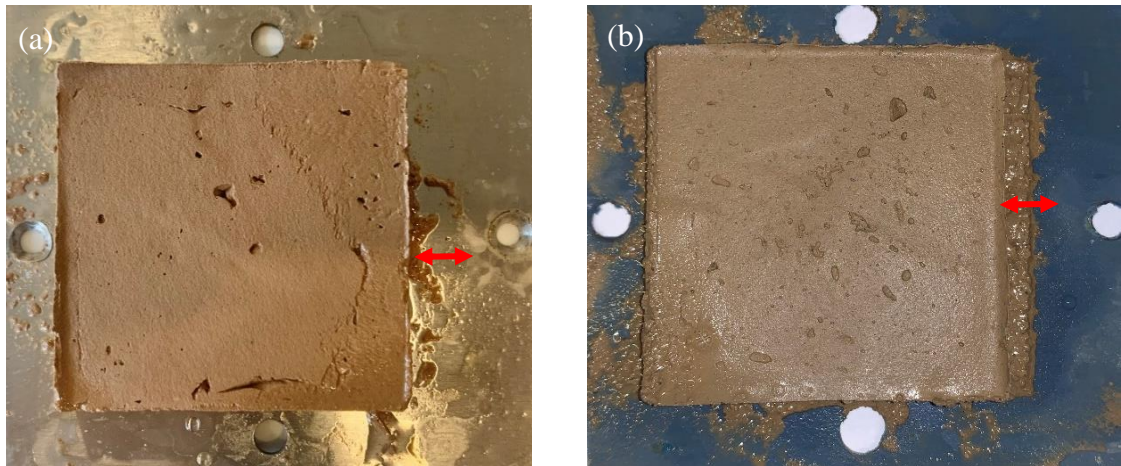


Figure 38 Failure mechanism of LPC on (a) Stainless steel and (b) Sandpaper

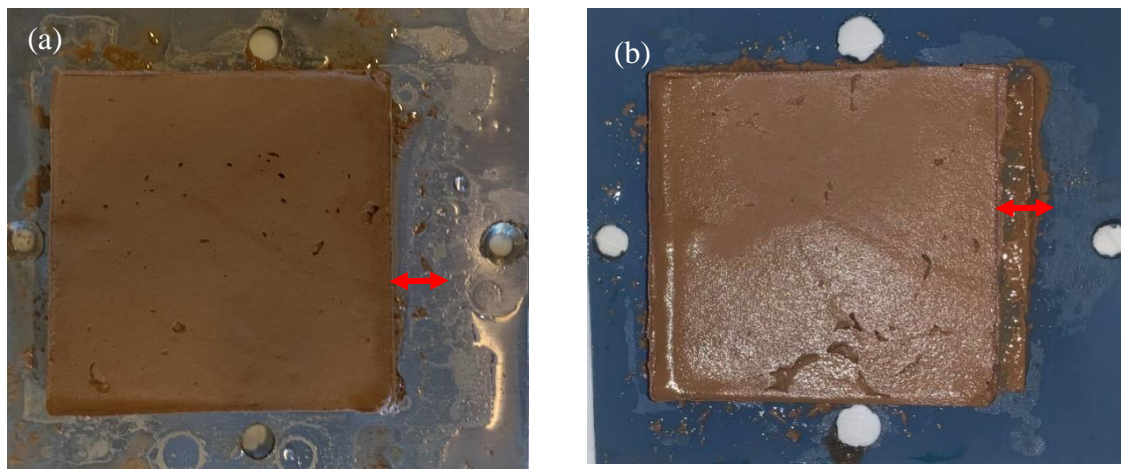


Figure 39 Failure mechanism of HPC on (a) Stainless steel and (b) Sandpaper

3. Effect of Clay Plasticity and Temperature on the Residual Friction Angle

Given that offshore pipelines are expected to exhibit significant deformations during the design life of the offshore facility, the design of the pipelines is usually governed by the drained residual interface friction angle between the pipeline material and the surrounding clay. **Figure 40** shows a comparison between the residual friction angles

measured for LPC and HPC at ambient and elevated temperatures. The curves are shown on the same graph to allow for meaningful comparisons.

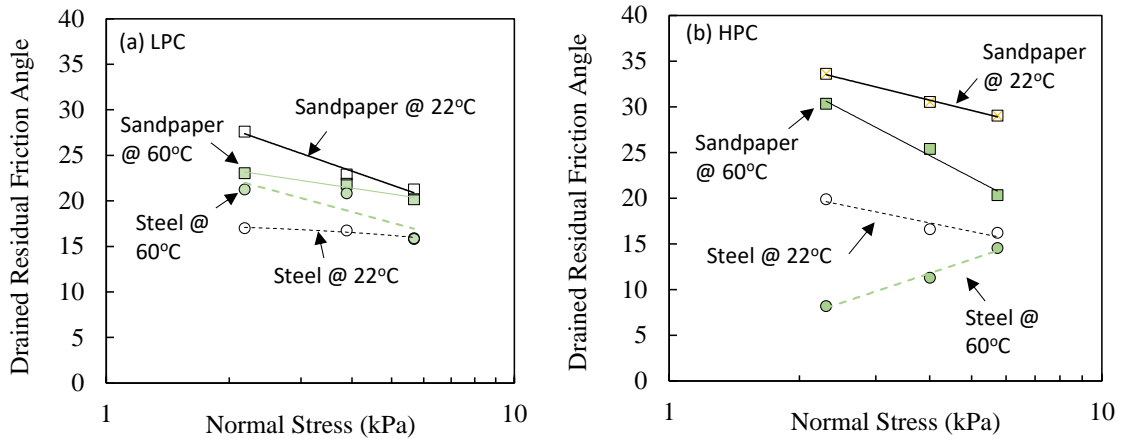


Figure 40 Residual Secant Friction Angle for (a) LPC and (b) HPC

Results on **Figure 40** indicate that the effect of heating the interface to a temperature of 60°C is to reduce the drained residual friction angle for LPC with the rough interface and HPC with the smooth and rough interface. For the case involving LPC with the smooth interface, the residual friction angle exhibited a slight increase at normal stresses that are low.

Moreover, results on **Figure 40** indicate that in most of the tests, the residual friction angle was found to be very sensitive to increases in temperature at relatively low normal stresses, with the sensitivity to temperature decreasing as the normal stress is increased to 6.1 kPa. The only exception is the tests conducted with HPC and the rough interface where elevated temperatures produced a relatively brittle response with significant strain softening, leading to residual stresses that are much smaller at higher normal stresses and elevated temperatures.

These observations point to a relatively high degree of complexity in the interface response at relatively high temperatures which is clearly affected by several factors that need to be investigated in future work. The results presented in this study

constitute a strong basis for designing experimental testing programs that are targeted towards isolating the effect of plasticity, surface roughness, and normal stress on the drained residual strength of pipe-clay interfaces.

CHAPTER V

CONCLUSIONS

The pipe-soil interface resistance is a key parameter in the design of HPHT pipelines. This study aimed at investigating the impact of elevated temperature on the interface response between clays and the pipeline coating. Tests were conducted at ambient (22°C) and elevated temperatures (60°C) to achieve the goals of the study. The following conclusions can be drawn from a total of 24 interface direct shear tests that were conducted on low and high plasticity clays tested against smooth stainless steel and rough sandpaper interfaces at normal stresses between 2.45 and 6.1 kPa:

1. The interface direct shear response at low normal stresses is highly sensitive to the magnitude of the normal stress, clay plasticity, interface roughness, and magnitude of the applied displacement (peak versus residual).
2. The drained interface peak and residual failure envelopes were nonlinear in the small pressure range. Heating the interfaces to 60°C had a variable effect on the interface response of LPC and HPC clays. Similarly, the temperature effect was variable depending on whether the interface tests were conducted with the smooth or rough interface. These results indicate that the drained response of clay-solid interfaces is a complex phenomenon when tested in the small pressure range.
3. For LPC tested with the smooth interface, heating the interface to 60°C increased the peak friction angle by 5.50°, 2.50°, and 0.50° at normal stresses of 2.45 kPa, 4.26 kPa, and 6.1 kPa, respectively. On the other hand, heating the rough interface to 60°C decreased the peak friction angle by 4.50, 1.50, and 1.0 degrees. It could be concluded from the LPC results that for very shallow pipe embedment (normal

stress of about 2 kPa), significant differences in the interface response is observed at elevated temperature. As the normal stress increases and approaches 6 kPa (pipe embedment increases), the effect of temperature on the interface response vanishes.

4. Unlike the LPC tests, results for HPC showed a very marked decrease in peak and residual stresses for the smooth interface at elevated temperature, particularly at small normal stresses. On the other hand, results of the rough interface tests indicated that elevated temperature did not have a significant effect on the peak shear stress, but resulted in significant reductions in the residual stress at large deformations, particularly for the case involving normal stresses of 6.1 kPa.
5. For the smooth interface and HPC, reductions in the order of 8.7° , 3.0° , and 0° were observed in the peak friction angle due to elevated temperature for normal stresses of 2.45 kPa, 4.26 kPa, and 6.1 kPa, respectively. The respective decreases in the residual friction angle were 11.7° , 5.3° , and 1.6° . For the rough interface, heating increased the peak friction angle by 4.3° , 1.8° , and 0° while the residual friction angles were reduced by 3.3° , 5.0° , and 9° , respectively due to heating.
6. Given that the residual strength typically governs the design of pipelines in the offshore environment, it could be concluded based on the tests conducted in this research that the effect of heating the interface to a temperature of 60°C is to reduce the drained residual friction angle for LPC with the rough interface and HPC with the smooth and rough interfaces. For the case involving LPC with the smooth interface, the residual friction angle exhibited a slight increase at normal stresses that are low. The residual friction angle was found to be very sensitive to increases in temperature at relatively low normal stresses, with the sensitivity to temperature decreasing as the normal stress is increased to 6.1 kPa.

REFERENCES

- AMERICAN SOCIETY FOR TESTING AND MATERIALS. (2000). D2487: Standard Practice for Classification of Soils for Engineering Purposes (Unified Soil Classification System). *GP, GM, SW, SP, and SM, or a Combination of These Groups, 04*, 1–12.
- ASTM D 3080. (2003). ASTM D 3080 - 03 Direct Shear Test of Soils Under Consolidated Drained Conditions. *ASTM International, 04*, 7. www.astm.org
- Bai, Y., Niedzwecki, J. M., & Sanchez, M. (2014). Numerical investigation of thermal fields around subsea buried pipelines. *Proceedings of the International Conference on Offshore Mechanics and Arctic Engineering - OMAE, 6B*(July 2015).
<https://doi.org/10.1115/OMAE2014-24678>
- Ballard, J.-C., & Jewell, R. (2013). Observations of pipe-soil response from in-situ measurements. *Proc. Of Offshore Technology Conference, 6–9 May 2013, Houston, Texas, USA, OTC 24154*. <https://doi.org/10.4043/24154-ms>
- Boukpeti, N. Ñ., & White, D. J. Ñ. (2016). *Interface shear box tests for assessing axial pipe – soil resistance. June 2015*.
- Boulon, M. (1989). Basic features of soil structure interface behaviour. *Computers and Geotechnics, 7*(1–2), 115–131. [https://doi.org/10.1016/0266-352X\(89\)90010-4](https://doi.org/10.1016/0266-352X(89)90010-4)
- Boylan, N., & White, D. J. (2014). *Seabed Friction On Carbonate Soils : Physical Modelling of Axial Pipe-Soil Friction OTC-25398-MS Seabed Friction On Carbonate Soils : Physical Modelling of Axial Pipe-Soil Friction. May*.
<https://doi.org/10.4043/25398-MS>
- Brier, C. De, Geoconsulting, J. B. F., & A, D. C. T. S. (2016). *On the added value of advanced interface shear testing for pipeline walking mitigation. 1–15*.

- Cekerevac, C., & Laloui, L. (2004). Experimental study of thermal effects on the mechanical behaviour of a clay. *International Journal for Numerical and Analytical Methods in Geomechanics*, 28(3), 209–228.
<https://doi.org/10.1002/nag.332>
- Chen, X., Zhang, J., Xiao, Y., & Li, J. (2015). Effect of roughness on shear behavior of red clay-concrete interface in large-scale direct shear tests. *Canadian Geotechnical Journal*, 52(8), 1122–1135. <https://doi.org/10.1139/cgj-2014-0399>
- DeJong, J. T., Randolph, M. F., & White, D. J. (2003). Interface load transfer degradation during cyclic loading: A microscale investigation. *Soils and Foundations*, 43(4), 81–93. https://doi.org/10.3208/sandf.43.4_81
- Delage, P., Cui, Y. J., & Tang, A. (2010). Clays in radioactive waste disposal Clays in radioactive waste disposal. *Journal of Rock Mechanics and Geotechnical Engineering*, 2(June), 111–123. <https://doi.org/10.3724/SP.J.1235.2010.00111>
- Di Donna, A., Ferrari, A., & Laloui, L. (2016). Experimental investigations of the soil–concrete interface: Physical mechanisms, cyclic mobilization, and behaviour at different temperatures. *Canadian Geotechnical Journal*, 53(4), 659–672.
<https://doi.org/10.1139/cgj-2015-0294>
- Eid, H. T., Amarasinghe, R. S., Rabie, K. H., & Wijewickreme, D. (2015). *Residual shear strength of fine-grained soils and soil – solid interfaces at low effective normal stresses*. 210(January 2014), 198–210.
- Hanson, J. L., Flores, A., Manheim, D., & Yesiller, N. (2015). *Temperature Effects on Sand-Steel Interface Shear and Quantification of Post-Shear Surface Texture Characteristics of Steel*. 1711–1720. <https://doi.org/10.1061/9780784479087.155>
- Hill, A. J., & Jacob, H. (2008). In-Situ Measurement of Pipe-Soil Interaction in Deep

- Water. *Proc. Of Offshore Technology Conference, 5–8 May 2008, Houston, Texas, U.S.A, OTC 19528*. <https://doi.org/10.4043/19528-ms>
- Houhou, R., Awad, A., Sadek, S., & Najjar, S. (2018). *Effect of Heating and Cooling Cycles on the Skin Friction of Energy Piles in Soft Clays*. 653–663.
<https://doi.org/10.1061/9780784481578.062>
- Hu, L., & Pu, J. (2004). Testing and Modeling of Soil-Structure Interface. *Journal of Geotechnical and Geoenvironmental Engineering*, 130(8), 851–860.
[https://doi.org/10.1061/\(asce\)1090-0241\(2004\)130:8\(851\)](https://doi.org/10.1061/(asce)1090-0241(2004)130:8(851))
- Li, C., Kong, G., Liu, H., & Abuel-Naga, H. (2019). Effect of temperature on behaviour of red clay–structure interface. *Canadian Geotechnical Journal*, 56(1), 126–134.
<https://doi.org/10.1139/cgj-2017-0310>
- Li, H., Kong, G., & Yang, Q. (2020). Thermal effects on the dynamic properties of marine sediment under long-term low cyclic stress. *Applied Ocean Research*, 104(September), 102361. <https://doi.org/10.1016/j.apor.2020.102361>
- Maghsoodi, S., Cuisinier, O., & Masrouri, F. (2019). Thermo-mechanical behaviour of clay-structure interface. *E3S Web of Conferences*, 92, 1–6.
<https://doi.org/10.1051/e3sconf/20199210002>
- Najjar, S. S., Gilbert, R. B., Liedtke, E., McCarron, B., & Young, A. G. (2007). Residual Shear Strength for Interfaces between Pipelines and Clays at Low Effective Normal Stresses. *Journal of Geotechnical and Geoenvironmental Engineering*, 133(6), 695–706. [https://doi.org/10.1061/\(asce\)1090-0241\(2007\)133:6\(695\)](https://doi.org/10.1061/(asce)1090-0241(2007)133:6(695))
- Najjar, Shadi S, Gilbert, R. B., Hall, C., & Mccarron, B. (2003). *Omae2003- 37499*. 1–8.

- Ozgener, O., Ozgener, L., & Tester, J. W. (2013). A practical approach to predict soil temperature variations for geothermal (ground) heat exchangers applications. *International Journal of Heat and Mass Transfer*, 62(1), 473–480.
<https://doi.org/10.1016/j.ijheatmasstransfer.2013.03.031>
- Pedersen, R. C., Olson, R. E., & Rauch, A. F. (2019). *Shear and Interface Strength of Clay at Very Low Effective Stress*. 26(1), 71–78.
- Randolph, M. F., White, D. J., & Yan, Y. (2012). Modelling the axial soil resistance on deep-water pipelines. *Géotechnique*, 62(9), 837–846.
<https://doi.org/10.1680/geot.12.OG.010>
- Rouaiguia, A. (2010). Residual shear strength of clay-structure interfaces. *International Journal of Civil & Environmental Engineering IJCEE-IJENS*, 10(03).
- Shakir, R. R., & Zhu, J. (2009). Behavior of compacted clay-concrete interface. *Frontiers of Architecture and Civil Engineering in China*, 3(1), 85–92.
<https://doi.org/10.1007/s11709-009-0013-6>
- Shi, Y., Wang, N., Gao, F., Qi, W., & Wang, J. (2019). Physical modeling of the axial pipe-soil interaction for pipeline walking on a sloping sandy seabed. *Ocean Engineering*, 178(November 2018), 20–30.
<https://doi.org/10.1016/j.oceaneng.2019.02.059>
- Skempton, A. W. (1985). Residual strength of clays in landslides, folded strata and the laboratory. *Geotechnique*, 35(1), 3–18. <https://doi.org/10.1680/geot.1985.35.1.3>
- Stanier, S. A., White, D. J., Chatterjee, S., Brunning, P., & Randolph, M. F. (2015). A tool for ROV-based seabed friction measurement. *Applied Ocean Research*, 50, 155–162.
- Stark, T. D., & Eid, H. (1994). DRAINED RESIDUAL STRENGTH OF COHESIVE

- By Timothy D. Stark, 1 Associate Member, ASCE, and Hisham T. Eid, 2 Student Member, ASCE SOILS. *Journal of Geotechnical and Geoenvironmental Engineering ASCE*, 120(5), 856–871.
- Tsubakihara, Y., Kishida, H., & Nishiyama, T. (1993). Friction between cohesive soils and steel. *Soils and Foundations*, 33(2), 145–156.
https://doi.org/10.3208/sandf1972.33.2_145
- Uesugi, M., Kishida, H., & Tsubakihara, Y. (1988). Behavior of Sand Particles in Sand-Steel Friction. *Soils and Foundations*, 28(1), 107–118.
<https://doi.org/10.3208/sandf1972.28.107>
- Uesugi, M., Kishida, H., & Tsubakihara, Y. (1989). Friction between sand and steel under repeated loading. *Soils and Foundations*, 29(3), 127–137.
https://doi.org/10.3208/sandf1972.29.3_127
- Uesugi, M., & Kishida, H. (1987). Frictional Resistance At Yield Between. *Soils and Foundations*, 26(4), 139–149. <https://doi.org/10.3208/sandf1972.26.4>
- Wang, D., Lu, L., & Cui, P. (2018). Simulation of thermo-mechanical performance of pile geothermal heat exchanger (PGHE) considering temperature-depend interface behavior. *Applied Thermal Engineering*, 139(July 2017), 356–366.
<https://doi.org/10.1016/j.applthermaleng.2018.02.020>
- Westgate, Z. J., White, D. J., & Savazzi, M. (2018a). Experience with interface shear box testing for axial pipe-soil interaction assessment on soft clay. *Proceedings of the Annual Offshore Technology Conference*, 3, 1565–1588.
<https://doi.org/10.4043/28671-ms>
- Westgate, Z. J., White, D. J., & Savazzi, M. (2018b). *OTC-28671-MS Experience with Interface Shear Box Testing for Axial Pipe-Soil Interaction Assessment on Soft*

Clay.

- Xiao, S., Suleiman, M. T., Elzeiny, R., Xie, H., & Al-Khawaja, M. (2017). *Soil-Concrete Interface Properties Subjected to Temperature Changes and Cycles Using Direct Shear Tests*. 175–183. <https://doi.org/10.1061/9780784480472.018>
- Yavari, N., Tang, A. M., Pereira, J. M., & Hassen, G. (2016). Effect of temperature on the shear strength of soils and the soil–structure interface. *Canadian Geotechnical Journal*, 53(7), 1186–1194. <https://doi.org/10.1139/cgj-2015-0355>
- Yazdani, S., Helwany, S., & Olgun, G. (2019). Influence of temperature on soil–pile interface shear strength. *Geomechanics for Energy and the Environment*, 18, 69–78. <https://doi.org/10.1016/j.gete.2018.08.001>
- Yin, K., Fauchille, A.-L., Di Filippo, E., Kotronis, P., & Sciarra, G. (2021). A Review of Sand–Clay Mixture and Soil–Structure Interface Direct Shear Test. *Geotechnics*, 1(2), 260–306. <https://doi.org/10.3390/geotechnics1020014>